Theoretical Notes
Note 79

SC-RR-70-216

MODELS FOR ELECTROMAGNETIC PULSE PRODUCTION FROM UNDERGROUND NUCLEAR EXPLOSIONS

PART I: Metallic Casing Effects

C. N. Vittitoe, 5231
Sandia Laboratories, Albuquerque

April 1970

ABSTRACT

A model is developed to estimate the electromagnetic pulse produced by a completely enclosed underground burst employing a metal cylindrical casing extending from the burst point to very near the earth's surface.

This research was supported by the Advanced Research Projects Agency of the Department of Defense under ARPA Order No. 1424.

Key words: Electric field intensity, current-generation mechanisms

b

ACKNOWLEDGMENTS

Helpful discussions with Albert Petschek and John Malik are gratefully acknowledged. Influence from the EMP community and especially some work of Louis Wouters is also appreciated. Steve Sherman wrote the major portion of the Antn computer program for the underground antenna model, with the aid of Ron Halbgewachs who furnished the subroutine for evaluating Bessel and Hankel functions for complex arguments. Several discussions with Rondall Jones and Ralph Partridge concerning the Fast Fourier Transform program are also acknowledged.

TABLE OF CONTENTS

MODELS FOR ELECTROMAGNETIC PULSE PRODUCTION FROM UNDERGROUND NUCLEAR EXPLOSIONS

I. INTRODUCTION AND OUTLINE

Underground testing of nuclear weapons has become commonplace since the atmospheric test ban treaty was signed. In such situations, the asymmetries attributable to air-earth interfaces, air density gradients, and geomagnetic field effects that are responsible for much of the EMP from bursts above ground, are not very effective in producing an electromagnetic pulse. Underground bursts introduce their own set of asymmetries in gamma ray absorption and resultant Compton electron current. These asymmetries create an EMP. The actual geometry associated with such a burst is extremely involved. Nevertheless, for certain types, simplifying assumptions enable models to be formulated. The following sections discuss essentially three generalized mechanisms for radioflash creation for the special burst types:

1. Burst with an evacuated line-of-sight pipe to the air-earth interface.
2. Burst with a metal, cylindrical casing surrounding the weapon, extending to ground zero, and filled with a lossy dielectric material.

The mechanisms are gamma column interaction with the air, the transmission line formed by the metallic casing and a bundle of wires at its center, and the casing reaction as an underground antenna.

Type 1 bursts are sometimes used to study interactions of the early radiation from the weapon with systems in a tower built over the hole. After a short time, the line of sight is closed to prevent violation of the test ban treaty. The type 2 bursts are usually for weapon development. The cased holes are typically filled with sand, gravel,

and grout, while surrounding materials may be concrete, iron, tuff, alluvium, and water. Generalized solutions to Maxwell's equations are developed in Section II for cylindrically symmetric geometries in the frequency domain. Wires usually connect weapon instrumentation up through the cased hole and along the ground to recording equipment. The configuration of a cased hole with a collection of wires near the center acts as a transmission line. This model, treated in Section III, is found not to be very effective in producing an EMP.

In order to calculate the fields radiated along the earth's surface, zeroth order assumptions are made; it is assumed that since tangential fields are continuous across a nonconducting interface, the fields on the earth's surface are not seriously changed by introduction of the air-earth interface. Contrary to results for propagation along thin horizontal wires or narrow slots in the interface, such an approximation appears reasonable for radiation from a vertical dipole.[1] With fields known on the boundary of the upper half space, Green's Theorem is then used in Section IV to calculate the fields everywhere in the upper half space.

A current can also exist on the casing itself. This situation, considered in Sections V and VI, can be produced by an antenna in a lossy, homogeneous earth. The vertical antenna current produces an azimuthal magnetic field and a radial electric field which act as sources for radiation into the upper half space. Most of the mathematical details are relegated to the appendices. Modeling for the type 1 bursts is treated in Part II of the report which will be published at a later date.

II. SOLUTION TO MAXWELL's EQUATIONS IN A CYLINDRICALLY SYMMETRIC CASE FOR A WAVE TRAVELING IN THE Z DIRECTION

Within a homogeneous, isotropic domain, Maxwell's equations in MKS units are given by

$$\begin{aligned} \nabla \times \underline{H} &= \underline{J} + \frac{\partial \vec{D}}{\partial t}, & \nabla \cdot \underline{D} &= \rho, \\ \nabla \times \underline{E} &= -\frac{\partial \vec{B}}{\partial t}, & \nabla \cdot \underline{B} &= 0. \end{aligned} \tag{1}$$

The time Fourier transform of these equations gives

$$\begin{aligned} \nabla \times \tilde{\underline{H}} &= \tilde{\underline{J}} - i\omega\tilde{\underline{D}}, & \nabla \cdot \tilde{\underline{D}} &= \tilde{\rho}, \\ \nabla \times \tilde{\underline{E}} &= i\omega\tilde{\underline{B}}, & \nabla \cdot \tilde{\underline{B}} &= 0, \end{aligned} \tag{2}$$

where

$$\tilde{V} = \tilde{V}(\omega) \equiv \frac{1}{2\pi} \int_{-\infty}^{\infty} V(t)\, e^{i\omega t} dt . \tag{3}$$

Assuming that the permittivity ϵ, permeability μ, and conductivity σ are constants, one obtains

$$\nabla \times \tilde{\underline{B}} = \mu\sigma\tilde{\underline{E}} - i\omega\mu\epsilon\tilde{\underline{E}} \tag{4}$$

and

$$\nabla \times \tilde{\underline{E}} = i\omega\tilde{\underline{B}} . \tag{5}$$

Combinations of these equations allow the field equations to be given in the form

$$\left[\nabla^2 + i\omega\mu\sigma + \omega^2 \mu\epsilon\right] \tilde{\underline{E}} = 0, \tag{6}$$

$$\left[\nabla^2 + i\omega\mu\sigma + \omega^2 \mu\varepsilon\right] \tilde{\underline{B}} = 0, \tag{7}$$

as occurs with Maxwell's equations in the time domain with an exp (- iωt) time dependence. Since the analysis is done entirely in the frequency domain, the ~ notation is now omitted.

Note that the Fourier transforms have assumed the conductivity, permeability, and permittivity of the transmission medium and are independent of frequency. These assumptions, so early in the treatment, seriously limit possibilities for extending the treatment to a more general case. However, a range of values may be considered which should put upper and lower limits on the transmitted field values. In addition, measurements of materials such as sand or earth at a wide range of frequencies are not generally available and are quite dependent upon conditions such as water content and actual composition.

For a traveling wave in the Z direction and assumed Z dependence of exp (ihZ) in cylindrical coordinates, we have

$$\left\{\frac{1}{r}\frac{\partial}{\partial r}\left(r\frac{\partial}{\partial r}\right) + \frac{1}{r^2}\frac{\partial^2}{\partial\theta^2} - h^2 + k^2\right\}\begin{pmatrix}\underline{E}\\ \\ \underline{B}\end{pmatrix} = 0, \tag{8}$$

where

$$k^2 \equiv \omega^2 \mu\varepsilon + i\omega\mu\sigma \ . \tag{9}$$

Let f be any component of $\underline{E}$ or $\underline{B}$. Then

$$\frac{1}{r}\frac{\partial}{\partial r}\left(r\frac{\partial f}{\partial r}\right) + \frac{1}{r^2}\frac{\partial^2 f}{\partial\theta^2} + \left(k^2 - h^2\right) f = 0 \ . \tag{10}$$

Applying separation of variables leads to

$$f = \sum_n \left\{ A_n J_n\left(\sqrt{k^2-h^2}\ r\right) + B_n N_n \left(\sqrt{k^2-h^2}\ r\right) \right\} e^{ihZ - i\omega t + in\theta}, \tag{11}$$

where J_n and N_n are the Bessel and Neumann functions of order n.

The Hertz vector $\vec{\pi}$ for a medium with no fixed polarization also obeys the above wave equation (10); hence, the field components are given by:[2]

$$\underline{E} = \nabla\nabla \cdot \vec{\pi} + \left(k^2 - h^2\right) \vec{\pi} \ ,$$
$$\underline{B} = \left(\sigma\mu - i\omega\mu\epsilon \right) \nabla \times \vec{\pi} \ . \tag{12}$$

For $r < a_1$, for example, in a region characterized by index (1),

$$E_r^{(1)} = \sum_{n=-\infty}^{\infty} \left[\frac{ih}{\lambda_1} J_n'(\lambda_1 r)\, a_n^{(1)} - \frac{\mu_1 \omega n}{\lambda_1^2 r} J_n(\lambda_1 r)\, b_n^{(1)} \right] F_n, \tag{13}$$

$$E_\theta^{(1)} = -\sum_{n=-\infty}^{\infty} \left[\frac{nh}{\lambda_1^2 r} J_n(\lambda_1 r)\, a_n^{(1)} + \frac{i\mu_1 \omega}{\lambda_1} J_n'(\lambda_1 r)\, b_n^{(1)} \right] F_n, \tag{14}$$

$$E_Z^{(1)} = \sum_{n=-\infty}^{\infty} J_n(\lambda_1 r)\, a_n^{(1)}\, F_n, \tag{15}$$

$$H_r^{(1)} = \sum_{n=-\infty}^{\infty} \left[\frac{nk_1^2}{\mu_1 \omega \lambda_1^2 r} J_n(\lambda_1 r)\, a_n^{(1)} + \frac{ih}{\lambda_1} J_n'(\lambda_1 r)\, b_n^{(1)} \right] F_n, \tag{16}$$

$$H_\theta^{(1)} = \sum_{n=-\infty}^{\infty} \left[\frac{ik_1^2}{\mu_1 \omega \lambda_1} J_n'(\lambda_1 r)\, a_n^{(1)} - \frac{nh}{\lambda_1^2 r} J_n(\lambda_1 r)\, b_n^{(1)} \right] F_n, \tag{17}$$

$$H_Z^{(1)} = \sum_{n=-\infty}^{\infty} \left[J_n(\lambda_1 r)\, b_n^{(1)} \right] F_n, \tag{18}$$

where $\lambda_1^2 = k_1^2 - h^2$ and $F_n = \exp(in\theta + ihZ - i\omega t)$. These expansions are given in Stratton,[2] where it is also pointed out that the symmetric mode is the only one expected to propagate in a solid conductor with azimuthal symmetry. Thus only n=0 is considered as we apply this treatment to a situation with a solid conductor at the center.

III. THE COAXIAL CABLE MODEL

Let space be divided into three regions as indicated in Fig. 1. Region 1 is a solid center conductor, region 2 is a dielectric, and region 3 is an outer, imperfect conductor. The current density in the center wire is

$$J_Z = \sigma_1 E_Z^{(1)} \quad , \tag{19}$$

yielding a total current

$$I = \int_0^{a_1} \int_0^{2\pi} J_Z r d\theta dr \quad , \tag{20}$$

$$= 2\pi \sigma_1 \int_0^{a_1} J_o (\lambda_1 r) a_o^{(1)} F_o r dr \quad ; \tag{21}$$

$$I = I_o e^{ihZ - i\omega t} \quad , \tag{22}$$

where

$$I_o = \frac{2\pi\sigma_1 a_1}{\lambda_1} a_o^{(1)} J_1(\lambda_1 a_1) \quad . \tag{23}$$

The n = 0 terms in the general equations in Section II can now be used to calculate the electromagnetic fields in the three regions of interest. Constants are evaluated from the boundary conditions. The mathematics for this calculation is given in Appendix A. For reasonable choices for physical parameters of the center conductor, dielectric, and lossy outer conductor, the main fields exist in the dielectric region. The z = 0 plane is now considered as excited by the fields calculated in Appendix A for region 2. These fields act as a source for radiation into the upper half space (z > 0), where no other sources are included. The excitation is in the interval $a_1 \leq r \leq a_2$ in the z = 0 plane. Note that two "z" coordinates are utilized; lower case z has its origin at the air-earth interface, while capital Z has its origin at the point of origin for the propagating wave.

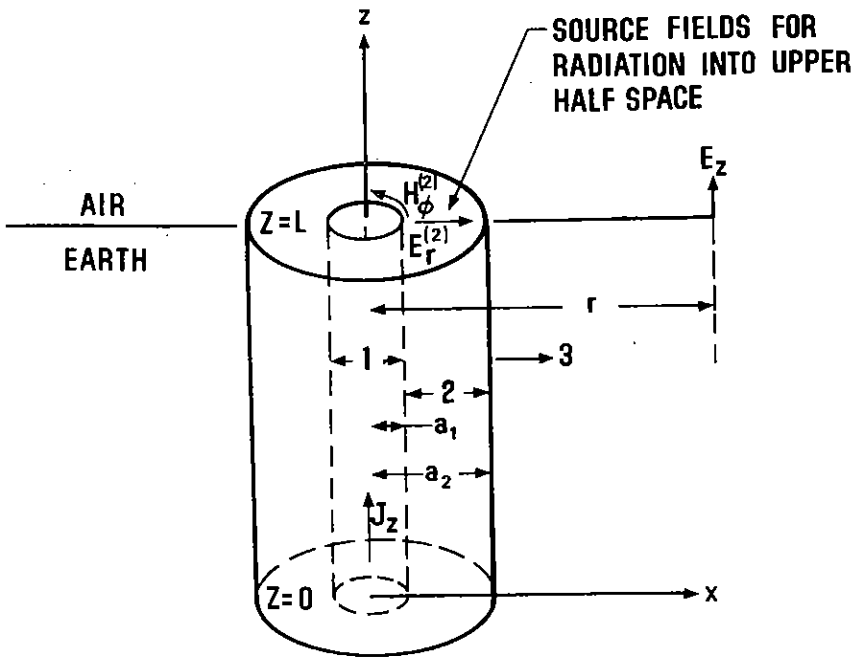

Fig. 1 The coaxial cable model.

Application of the Coaxial Cable Model to a Special Case

Consider the situation $a_1 \approx 0.10$ m, $a_2 \approx 1$m, $\sigma_1 = \sigma_3 = 10^7/\Omega m$, $\sigma_2 = 1.5\ 10^{-4}/\Omega m$, $\mu_1 = \mu_2 = \mu_3 = \mu_o$, $\epsilon_2 = 10\ \epsilon_o$. Then, from Appendix A,

$$k_2^2 = 111\ 10^{-18}\ \omega^2 + i\omega\ 18.8\ 10^{-11}\ , \tag{24}$$

with k_2 in m^{-1} and ω in sec^{-1}. Thus

$$\lambda_\ell \approx k_\ell = \sqrt{i\omega\mu_\ell\sigma_\ell}\ , \tag{25}$$

$$\lambda_1 a_1 \approx 0.35\ \sqrt{i\omega}\ , \tag{26}$$

$$\lambda_3 a_2 \approx 35.5\ \sqrt{i\omega}\ . \tag{27}$$

From Eq. (A-34),

$$h \approx k_2 \left[1 + \frac{i}{9.2\sqrt{\pi i\omega}} \left\{ \frac{H_o^{(1)}(35.5\sqrt{i\omega})}{H_1^{(1)}(35.5\sqrt{i\omega})} - 10\,\frac{J_o(0.35\sqrt{i\omega})}{J_1(0.35\sqrt{i\omega})} \right\} \right]. \quad (28)$$

For $\omega \geq 10^4$, $0.35\sqrt{\omega} \approx 35 >> 1$ and asymptotic values may be used for the cylindrical functions. These asymptotic values are most easily found by conversion to modified Bessel functions $I_\nu(x)$ and $K_\nu(x)$, which become independent of ν for large x:

$$\frac{H_o^{(1)}(35.5\sqrt{\frac{\omega}{i}}\,i)}{H_1^{(1)}(35.5\sqrt{\frac{\omega}{i}}\,i)} \to i, \quad \frac{J_o(0.35\sqrt{\frac{\omega}{i}}\,i)}{J_1(0.35\sqrt{\frac{\omega}{i}}\,i)} \to -i\,. \quad (29)$$

Thus

$$h \approx k_2 \left[1 - \frac{11}{9.2\sqrt{\pi i\omega}} \right]. \quad (30)$$

At frequencies larger than 10^4 Hz, the correction term to h is indeed small. Also

$$\lambda_2^2 = k_2^2 - h^2 = k_2^2 \left(\frac{22}{9.2\sqrt{\pi i\omega}} \right). \quad (31)$$

From (A-36), the magnetic field may now be written

$$H_\theta(2) = \frac{2ik_2^2\,B}{\pi\omega\mu_2\,\lambda_2^2} \left\{ \frac{ik_2^2}{2\mu_2}\sqrt{\frac{\mu_1 i}{\omega\sigma_1}}\,\frac{r}{a_1} + \frac{1}{r} \right\} \exp\left[ik_2 Z - i\omega t \right]. \quad (32)$$

For the parameter values chosen, with r varying between 0.1 and 1m, the 1/r term dominates unless frequency is greater than 10^{10} Hz. Therefore, Eq. (32) becomes

$$H_\theta(2) = \frac{2ik_2^2\,B}{\pi\omega\mu_2\,\lambda_2^2}\,\frac{\exp\left[ik_2 Z - i\omega t\right]}{r}\,. \quad (33)$$

With B approximated by (A-24), one obtains

$$H_\theta^{(2)} = \frac{I}{2\pi r} \quad , \tag{34}$$

as in the infinite conductivity situation. As Stratton[2] points out, such a result indicates that the displacement and conduction currents in the dielectric are much smaller than the conduction current in the inner conductor.

The attenuation comes from the propagation factor

$$h = k_2 \left[1 - \frac{11}{9.2\sqrt{\pi i \omega}} \right]. \tag{35}$$

With the assumption that $\omega > 10^4$ Hz, so that the correction term may be neglected,

$$h^2 = k_2^2 = 111\ 10^{-18}\ \omega^2 + i\omega\ 18.8\ 10^{-11} \tag{36}$$

$$= \mu_2\ \epsilon_2\ \omega^2 + i\mu_2\sigma_2\omega \quad . \tag{37}$$

The real and imaginary parts are

$$\left.\begin{matrix} k_r \\ k_i \end{matrix}\right\} = \sqrt{\mu_2\epsilon_2}\ \omega \left[\frac{\sqrt{1 + \left\{\frac{\sigma_2}{\epsilon_2\omega}\right\}^2} \pm 1}{2} \right]^{1/2} \tag{38}$$

or

$$\left.\begin{matrix} k_r \\ k_i \end{matrix}\right\} = 7.4\ 10^{-9}\ \omega \left[\sqrt{1 + \left\{\frac{1.7\ 10^6}{\omega}\right\}^2} \pm 1 \right]^{1/2} \quad , \tag{39}$$

where MKS units are used throughout.

As in (A-9) and (A-10), the electric field components are

$$E_r^{(2)} = \frac{\omega\mu_2 \, h}{k_2^2} H_\theta^{(2)} \quad , \tag{40}$$

$$E_Z^{(2)} = - \frac{\omega\mu_2 \, \lambda_2}{ik_2^2} \frac{AJ_o(\lambda_2 r) + B \, N_o(\lambda_2 r)}{AJ_1(\lambda_2 r) + B \, N_1(\lambda_2 r)} H_\theta^{(2)} \quad . \tag{41}$$

These correspond to (A-25) and (A-26) with the correction term from finite conductivity.

The magnitude of the radial field radiation source term can be estimated from Eqs. (34) and (40):

$$E_r^{(2)} = \frac{\omega \, 4\pi \, 10^{-7} \, I_o \exp\left[ik_2 \, Z - i\omega t\right] k_2}{2\pi r \, k_2^2} \quad . \tag{42}$$

Let

$$k_2 = \omega(A_1 + iB_1), \tag{43}$$

where A_1 and B_1 are defined by comparison with (39). Then

$$E_r^{(2)} = \frac{2 \, 10^{-7} \, I_o \exp\left[i\omega(A_1 Z - t)\right] \exp\left[-\omega B_1 Z\right]}{(A_1 + iB_1) r} \; ; \tag{44}$$

$$\frac{r^2 \left|E_r^{(2)}\right|^2}{I_o(Z)^2} = \frac{365 \exp\left\{ - 14.8 \, 10^{-9} \, \omega Z \left[\sqrt{1 + \left\{\frac{1.7 \, 10^6}{\omega}\right\}^2} - 1\right]^{1/2}\right.}{\left[1 + \left\{\frac{1.7 \, 10^6}{\omega}\right\}^2\right]^{1/2}} \quad . \tag{45}$$

The $\frac{\left|E_r^{(2)}\right|^2 r^2}{I_o^2}$ is given as a function of ω in the following graph, Fig. 2.

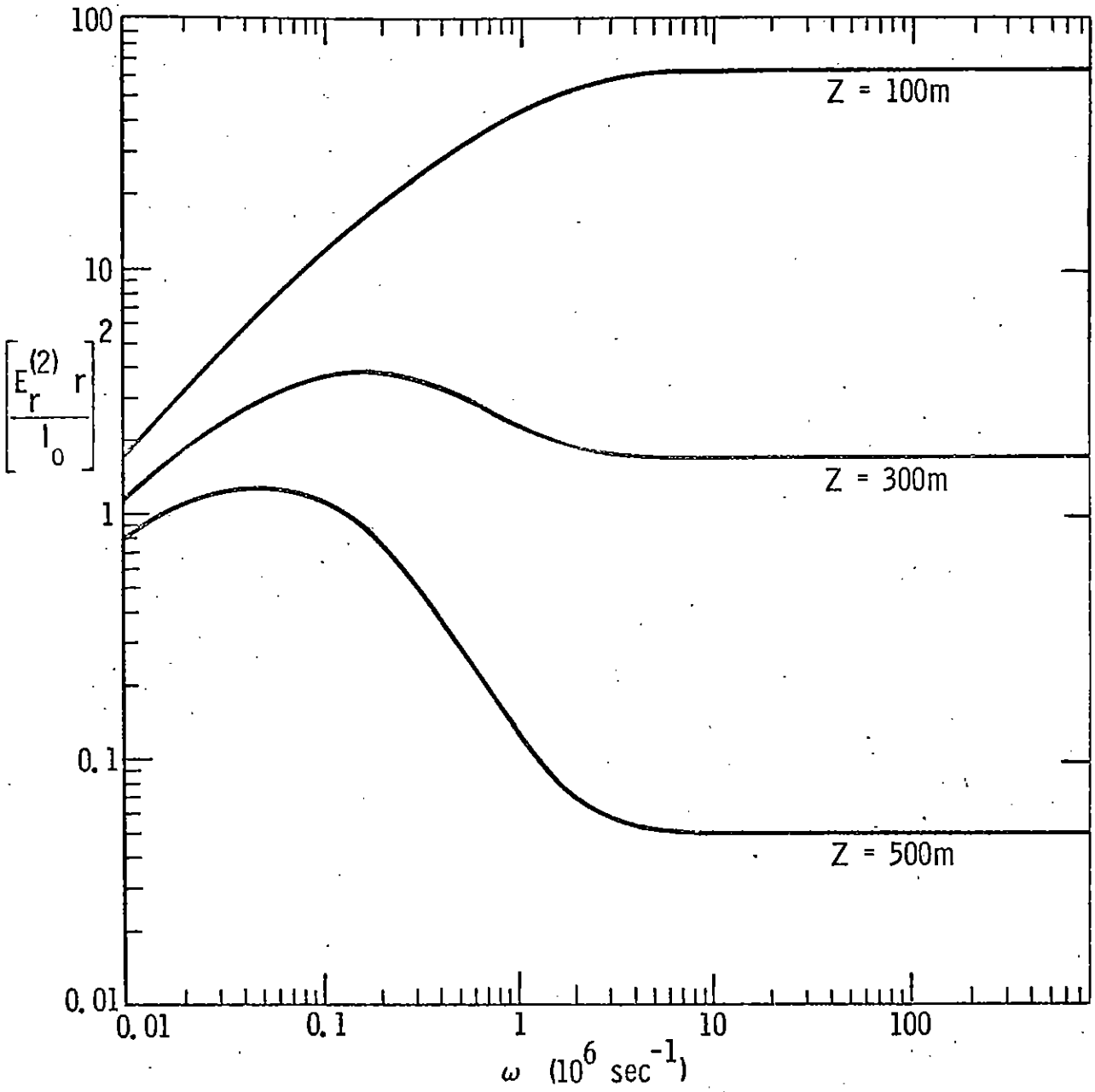

Fig. 2 Indication of frequency variation in radial electric field intensity in region 2 for selected distances of propagation by the coaxial cable model.

IV. THE DIFFRACTION MECHANISM FOR CONVERSION TO A RADIATING SIGNAL

Kirchhoff's diffraction theory gives the solution of the homogeneous wave equation at an arbitrary point in terms of the values of the solution and its first derivative at all points on an arbitrary closed surface surrounding the point.[3] This scalar wave approach is reasonable if the spatial discontinuities are small compared to the wavelengths of interest. If frequencies to 10^8 are considered, the minimum associated wavelength is 3 meters. Thus, scalar theory is stretched somewhat in application to the present example with an opening radius of 1 meter. Nevertheless, the Kirchhoff scalar theory is used, so some distortion will be obtained at the high frequencies.

The boundary conditions in the frequency domain are specified by Eqs. (34) and (44) for specific values of Z and $I_o(Z)$ in the special case chosen. This boundary, for $a_1 \leq r < a_2$, is then assumed to excite the free upper half space, producing radiation. Since the outer conductor was earlier chosen to be a reasonably good conductor, the radial and vertical components of electric field intensity are very small in region 3 and cannot contribute to the radiation in the upper half space.

Application of diffraction theory (see Appendix B) gives a radiating vertical electric field intensity

$$E_z = \frac{-Ge^{ikr}}{2r}\left[J_o(ka_2) - J_o(ka_1)\right], \tag{46}$$

where, in MKS units,

$$G = \frac{2 \times 10^{-7}\, I_o \exp\left[i\omega(A_1 Z - t)\right] \exp\left[-\omega B_1 Z\right]}{(A_1 + iB_1)} \tag{47}$$

and A_1 and B_1 are defined by (43).

Thus,

$$|E_z|^2 = \frac{|G|^2}{4r^2}\left[J_o(k\,a_2) - J_o(k\,a_1)\right]^2 . \tag{48}$$

At $\omega = 10^6$, $|G|^2 = 2\ I_o^2$ with the choices in the previous example, $a_2 = 1$, $a_1 = 0.1$, $Z = 300$,

$$k\ a_2 = \frac{\omega}{c}\ a_2 \approx 1/300 \quad , \tag{49}$$

$$k\ a_1 = \frac{0.1}{300} \quad , \tag{50}$$

and asymptotic forms may be used to calculate the difference in Bessel functions as $\sim 1/36 \times 10^4$. Thus

$$|E_z|^2 = \frac{I_o^2}{2r^2} \left[\frac{1}{36 \times 10^4}\right]^2 \quad . \tag{51}$$

With $r \approx 100$ meters,

$$|E_z| \approx \frac{I_o}{7.20}\ \mu V\ \text{sec/m} \tag{52}$$

in the frequency domain.

For $\omega = 10^8$, Eq. (46) becomes

$$|E_z| \approx \frac{I_o}{900}\ \text{V sec/m} \quad . \tag{53}$$

It appears that higher frequencies are preferentially transmitted in this model. The higher frequencies are transmitted more readily because of the greater difference in Bessel functions. However, the attenuation is much larger at such high frequencies.

In order to calculate the field in the time domain, let the current in the center wire be

$$I_o(Z,t) = I_1(Z)\ f\ (t). \tag{54}$$

Its Fourier transform is then

$$I_o(\omega,Z) \equiv I_1(Z)\ \tilde{f}\ (t). \tag{55}$$

Then, from inversion of (46),

$$E_z(t) = \int_{-\infty}^{\infty} E_z(\omega)\, e^{-i\omega t}\, d\omega. \tag{56}$$

A given form for $I_o(Z,t)$ and values of the various constants can then, in principle, be used to find the radiation fields predicted by this model.

Calculations have been performed with the assumed current

$$I_o(Z,t) = A\,[\exp(-bt) - \exp(-at)], \tag{57}$$

and the Fourier transform from Eq. (3),

$$I_o(\omega,Z) = \frac{A}{2\pi}\left[\frac{1}{a-i\omega} - \frac{1}{b-i\omega}\right]. \tag{58}$$

Parameters chosen were r = 100m, Z = 300m, $a = 2 \times 10^7$ sec^{-1}, $b = 10^7$ sec^{-1}, A determined by a peak current of 25 amperes, and other parameters as in the special case. Thus,

$$I_{peak} = A\left\{\exp\left[\frac{-b\ \ell n(b/a)}{b-a}\right] - \exp\left[\frac{-a\ \ell n(b/a)}{b-a}\right]\right\}. \tag{59}$$

The resulting vertical electric field had a peak value of the order of 10^{-9} volt/meter because of attenuation in the lossy dielectric filling the transmission line. Such a mechanism is poor for EMP production.

V. AN UNDERGROUND ANTENNA MODEL FOR EMP PRODUCTION

Let space be divided into two regions, as suggested in Fig. 3: Region I has $0 \leq r \leq a_1$ while region II has $r > a_1$. Here, r is the distance from the z axis in the cylindrical coordinate system. Region I is assumed to be a good conductor, while region II is the earth (which probably should not be referred to as ground). Azimuthal symmetry is assumed, so much of the earlier treatment applies.

The analysis given in Appendix C for this model includes calculation of the fields in region II and use of these fields on the $z = 0$ plane as sources for the diffraction problem analogous to that of Sections III and IV. As indicated in the following section, this model appears reasonably efficient in EMP production.

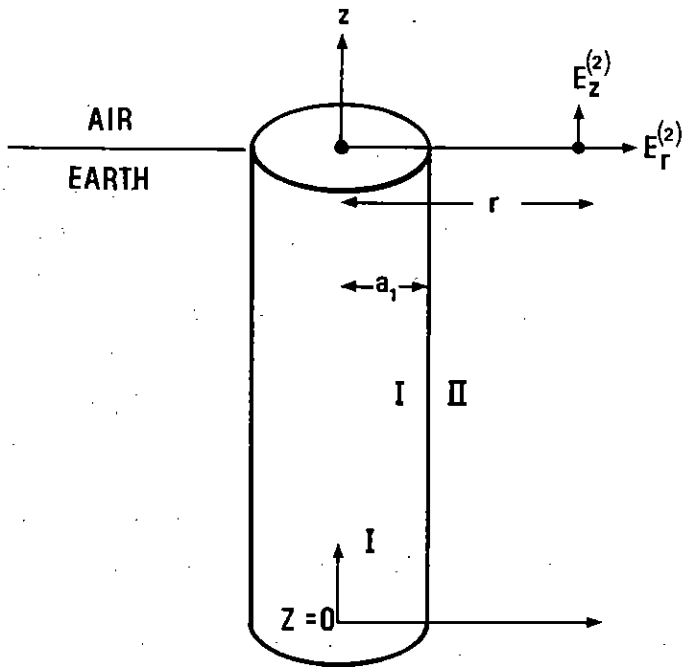

Fig. 3 The underground antenna model.

VI. RESULTS OF THE UNDERGROUND ANTENNA MECHANISM FOR A SPECIAL CASE

A computer program Antn was written to calculate signals for the underground antenna model described in Section V and Appendix C. For the illustration presented here, the current on the pipe casing was assumed to be given by Eq. (57) with a peak value of 25 amperes, $a = 2 \times 10^7$ sec^{-1}, and $b = 1 \times 10^7$ sec^{-1}, as in the special case considered earlier. The frequency domain representation was obtained from the Fast Fourier Transform Subroutine, FOURT.[4] The current and its transform are illustrated in Figs. 4 and 5. With the FOURT routine, the time interval considered (0 to 10 microseconds) and the number of sampled time points (4096) determine the frequency interval needed for calculations. The amplitude of I (ω) is artificially calculated for $\omega > 10^9$ sec^{-1} since, left to its own devices, the amplitude climbs sharply up to the low frequency value. Since this is above the Nyquist frequency, no real information is available in this frequency region.

The parameter λ_2 is found from solution of Eq. (C-20) with $a_1 = 1$m, $\sigma_1 = 10^7/(\text{ohm m})$, $\sigma_2 = 1.5 \times 10^{-4}$ ohm^{-1} m^{-1}, $\mu_1 = \mu_2 = \mu_o$, $\varepsilon_1 = \varepsilon_2 = \varepsilon_o$. The variation of λ_2 is graphed in Figs. 6 and 7 to check consistency and the approximation $|a_1\lambda_2| \ll 1$. The propagation constant is evaluated from Eq. (C-17) and graphed in Figs. 8 and 9. With the determination of these parameters, the vertical component of electric field intensity in the frequency domain is calculated from (C-41), with r = 100 m, Z = 300 m (see Fig. 10). The required Bessel and Hankel functions are obtained from the subroutine BESCOM.[5] The Fast Fourier Transform yields the time domain result in Fig. 11. Equation (C-34) gives the radial component of electric field intensity at this distance. These results are indicated in Figs. 12, 13, and 14.

Note that the 25-ampere peak current on the underground antenna in this example results in a 0.009 V/m peak vertical electric field intensity and 0.017 V/m peak radial component at 100 meters from ground zero. The relative magnitudes and amplitudes are expected to be particularly sensitive to the choices of earth conductivity and permittivity. This is considered in Appendix D.

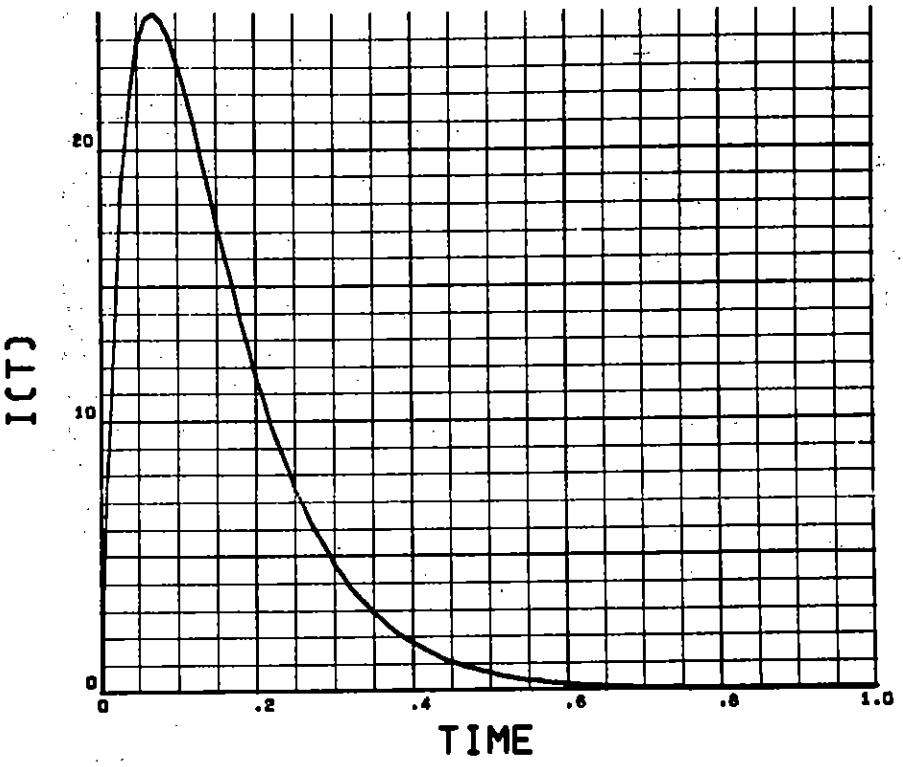

Fig. 4 The assummed current (amperes) as a function of time (microseconds).

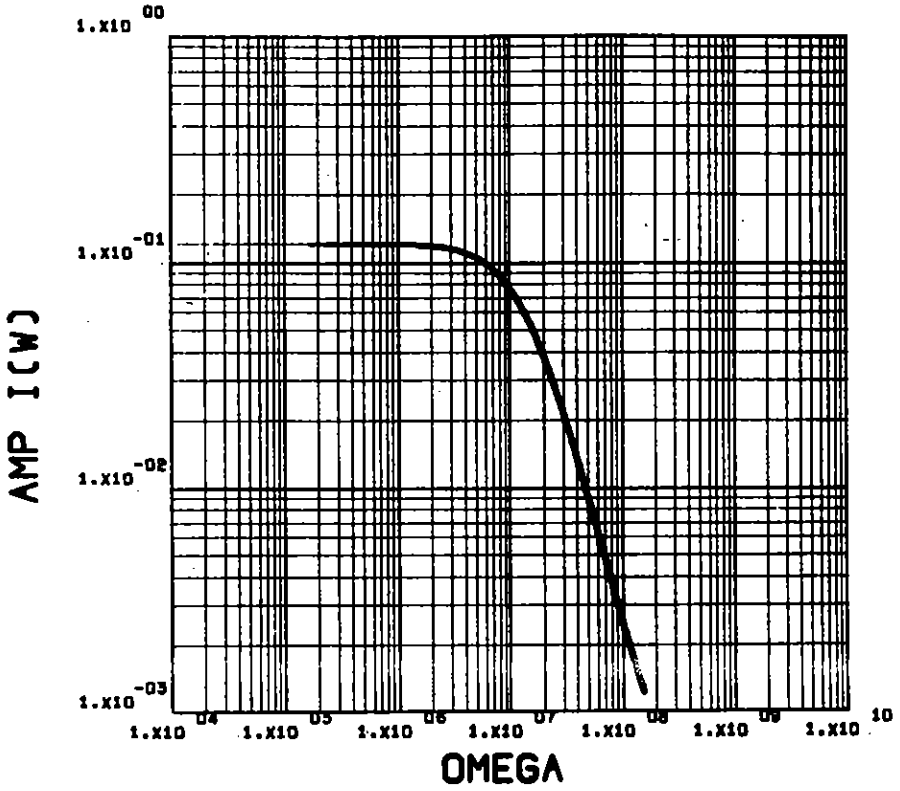

Fig. 5a Current amplitude (amp-sec) in the frequency domain.

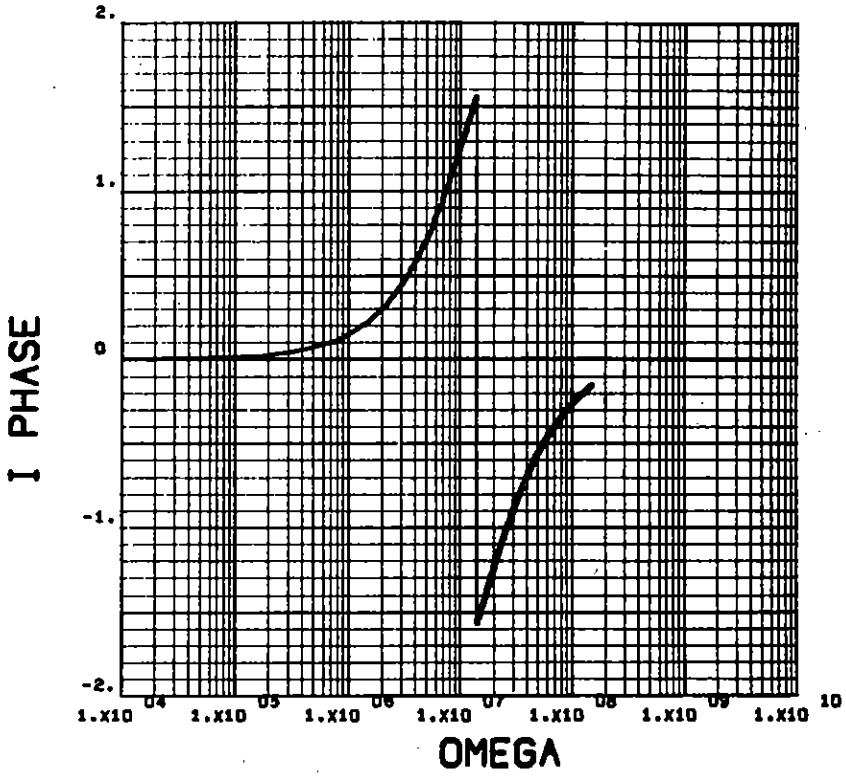

Fig. 5b Phase angle of the current in the frequency domain.

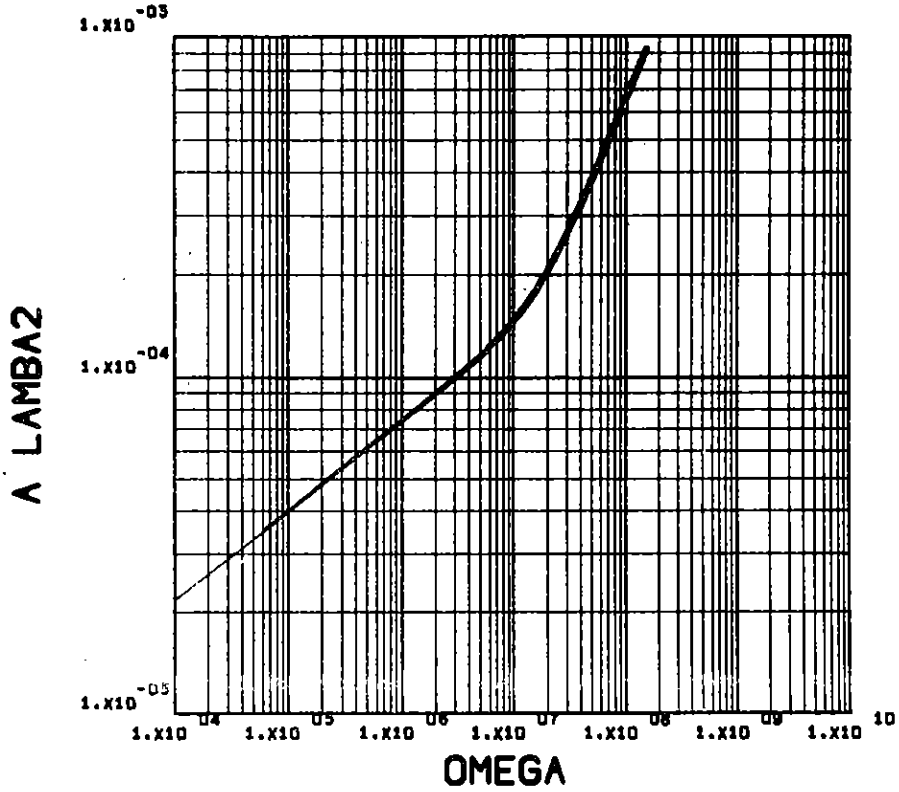

Fig. 6 Variation in the amplitude of λ_2 (m^{-1}).

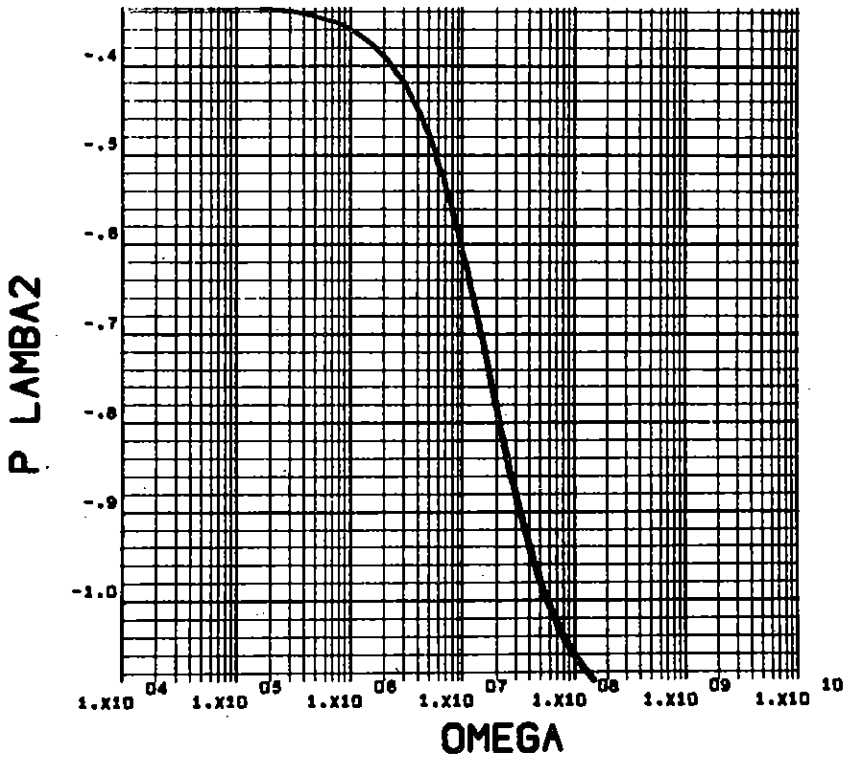

Fig. 7 Variation in the phase (radians) of λ_2.

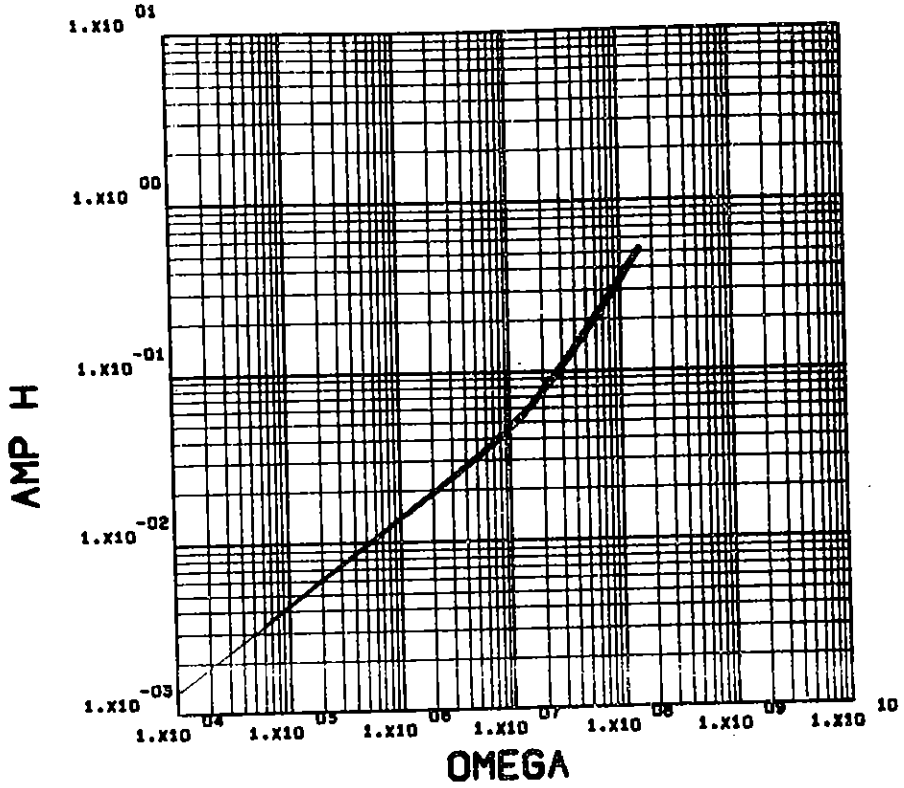

Fig. 8 Amplitude of the propagation constant (m^{-1}).

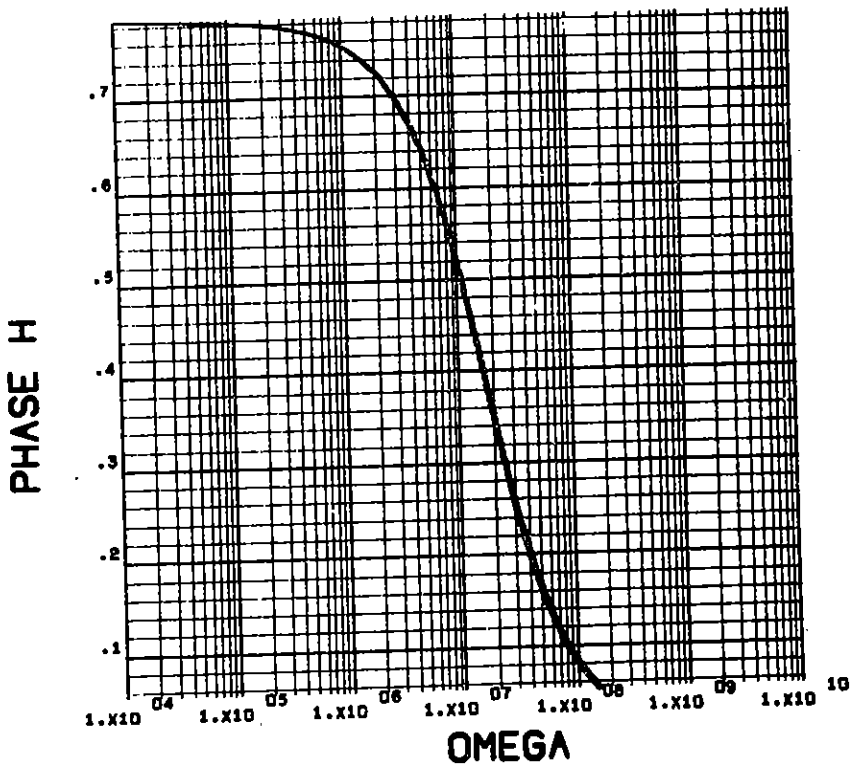

Fig. 9 Phase of the propagation constant (radians).

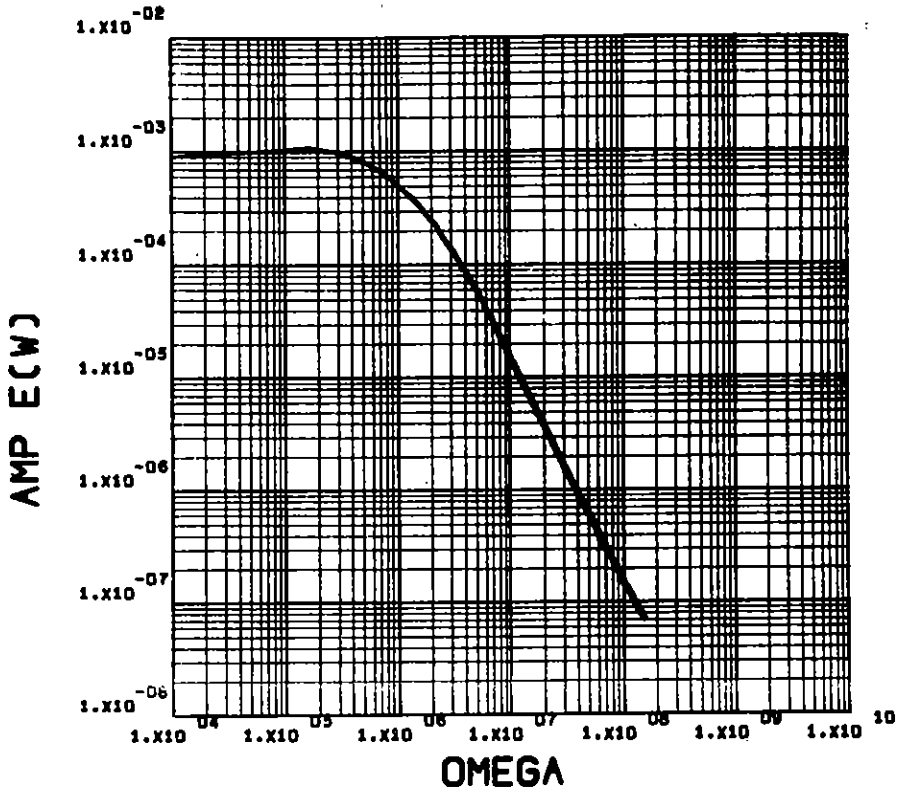

Fig. 10 Amplitude of the vertical electric field (V sec/m) in the frequency domain.

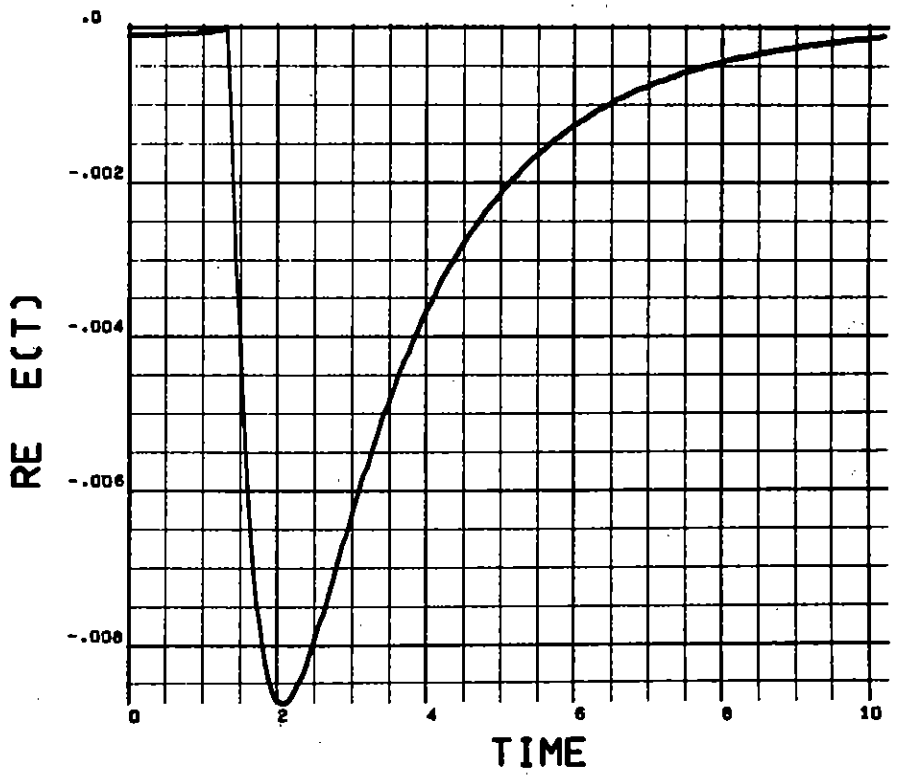

Fig. 11 The vertical electric field intensity (V/m) versus time (μsec) radiated to 100m from ground zero.

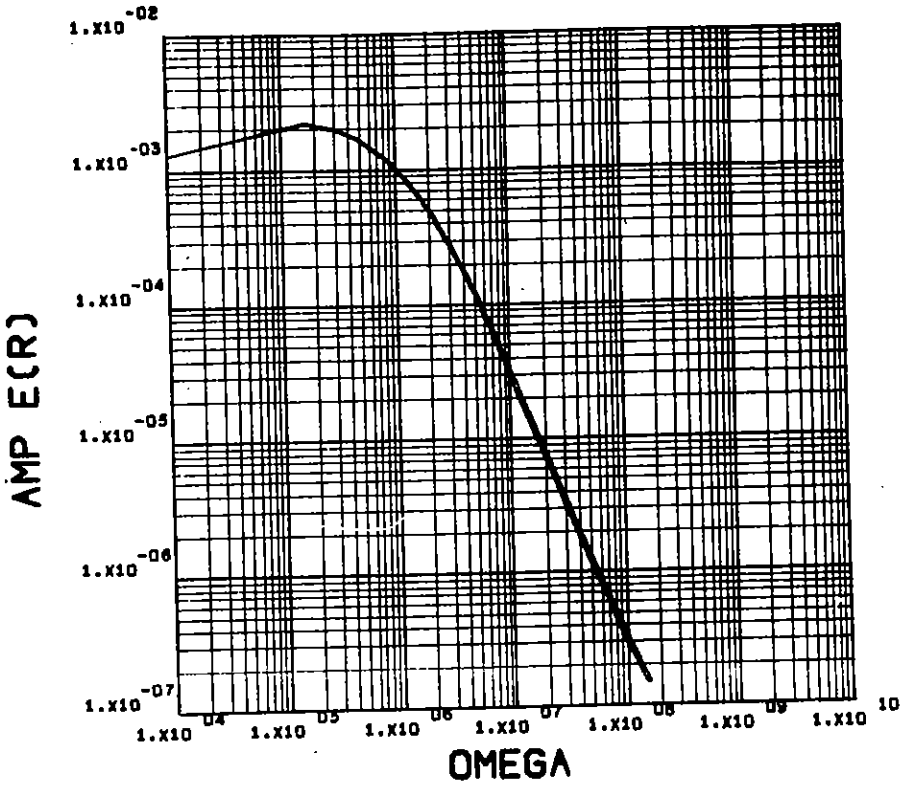

Fig. 12 Amplitude of the radial electric field (V sec/m) in the frequency domain.

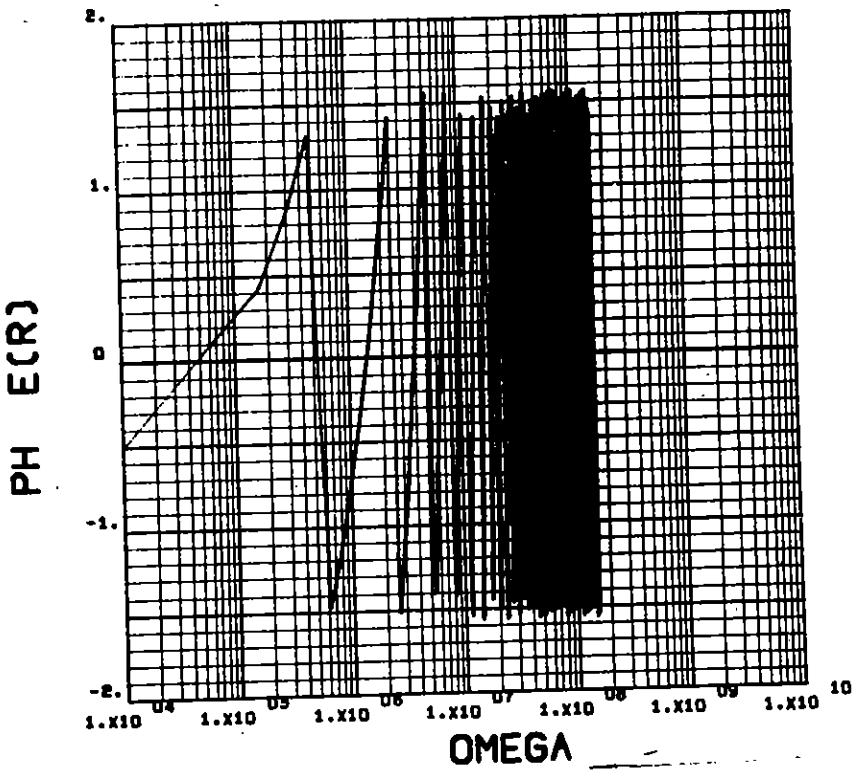

Fig. 13 Phase of the radial electric field intensity (radians) in the frequency domain.

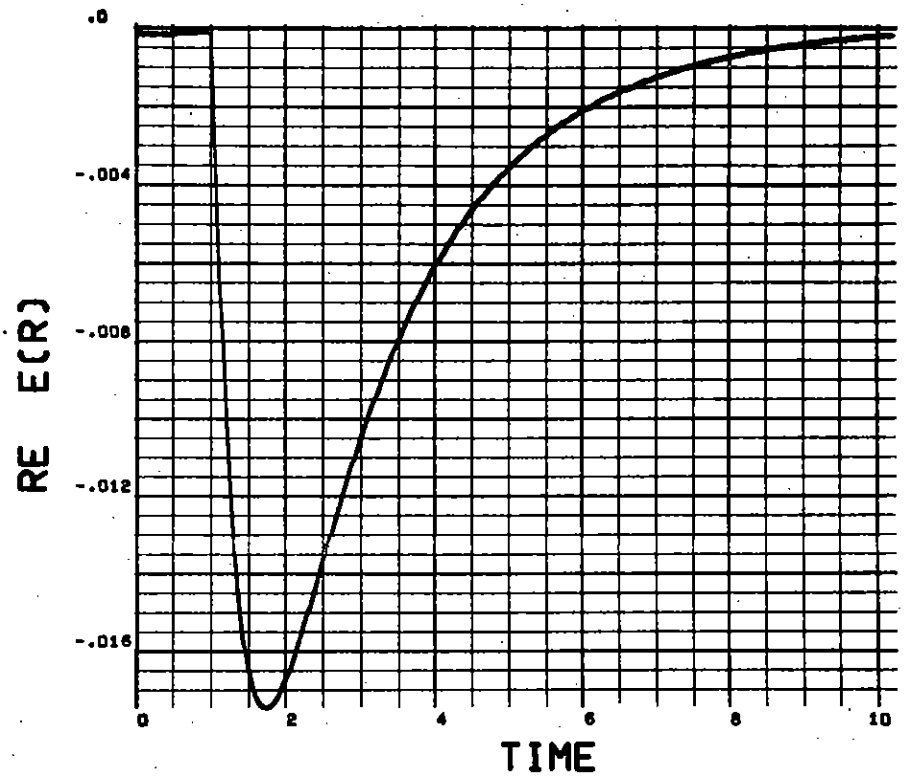

Fig. 14 The radial electric field intensity (V/m) versus time (μsec) at 100 m from ground zero.

VII. GENERAL DISCUSSION OF A POSSIBLE CURRENT-GENERATING MECHANISM

For an underground burst one might conclude that spherical symmetry in the absorption of gamma rays prevents radiating electromagnetic fields. The symmetry, coupled with the Gauss law, demands that the electric field intensity be zero outside the gamma ionization region. This suggests that no field is present to induce currents on the underground pipe encasing the weapon.

The charge displaced by a 1-kt weapon can be estimated by assuming 0.1 percent conversion to prompt gamma energy and 100 percent conversion of gamma rays to Compton electrons. The total electron charge generated is then near 4×10^3 coulombs. Since the ratio of electron mean free path to gamma ray mean free path is 0.01, only about 40 coulombs of charge are effectively separated. With the gamma mean free path near 10 cm, the effective charge separation distance must be at least 10 cm, while 1 meter appears as a reasonable lower limit. At 1 meter, for example, the integrated gamma flux should be of the order of 10^{13} γ/cm^2, sufficient to produce considerable ionization. The capacitance between two concentric conductors with dielectric constant ϵ_o separating them and radii 0.1 and 1 meter is about 10μμf. With 40 coulombs of charge on each sphere, the internal field strength is of the order of 4×10^{12} V/m, clearly too high for consistency. If Maxwell's equations were solved in the material, with Compton current as the source term, and breakdown of the material included, fields no larger than about 10^7 V/m are expected. It is likely that the effective capacitor radii are underestimated, while the charge is overestimated.

If it is assumed that the surrounding material is more dense directly above the burst than beneath it, an asymmetry is introduced, and nonzero fields can exist outside the source region. Instrumentation and support structure above the weapon could introduce such an asymmetry. If only 4 coulombs are assumed to be effectively separated by 1 meter, the field along the dipole axis is

$$E \approx \frac{Q\ell}{2\pi\epsilon r^3} .$$

With $r \approx 100$ m and $\epsilon = 10\,\epsilon_o$,

$$E \approx 7200 \text{ V/m} .$$

Of course, the physical situation is not static; sharpness of the current pulse indicates that high frequencies are involved. The field value will be reduced by skin depth effects as well as by the time required to produce the 4 coulombs of charge.

The skin depth is

$$\delta = \sqrt{\frac{2}{\omega\mu\sigma}} .$$

For $\omega = 10^6$ sec^{-1}, $\mu = \mu_o$, and $\sigma \approx 10^{-4}$ ohm^{-1} m^{-1}, typical of dry sands used to fill the pipe casings, $\delta = 110$ meters. For $\omega = 10^6$ and $\sigma \approx 10^{-3}$, typical of some Nevada soils, $\delta = 40$ meters. These skin depths indicate that a longitudinal electric field may exist at approximately 100 meters from the weapon because of an asymmetry in the weapon surroundings. Such a field would induce current in the pipe casing. This current is the source for the underground antenna model discussed in Section V. More detailed modeling of this current production mechanism is required for specific calculations of the propagating radioflash produced by a specific underground burst. However, such an underground antenna model must be retained as a reasonable radiating EMP production mechanism. Comparison of data with predictions from this model is planned for a future, classified report.

APPENDIX A

MATHEMATICAL DETAILS OF THE COAXIAL CABLE MODEL

APPENDIX A

MATHEMATICAL DETAILS OF THE COAXIAL CABLE MODEL

The generalized equations in Section II allow one to calculate the azimuthal component of the magnetic field intensity in region 1:

$$H_\theta^{(1)} = \frac{ik_1^2}{\mu_1 \omega \lambda_1} J_o'(\lambda_1 r)\, a_o^{(1)} \quad , \tag{A-1}$$

or, with the help of Eqs. (22) and (23),

$$H_\theta^{(1)} = -\frac{ik_1^2 I}{2\pi a_1 \omega \mu_1 \sigma_1} \frac{J_1(\lambda_1 r)}{J_1(\lambda_1 a_1)} \quad . \tag{A-2}$$

From the expansions in Stratton[2]

$$E_r^{(1)} = \frac{\omega \mu_1 h}{k_1^2} H_\theta^{(1)} \quad , \tag{A-3}$$

$$E_Z^{(1)} = -\frac{\omega \mu_1 \lambda_1}{ik_1^2} \frac{J_o(\lambda_1 r)}{J_1(\lambda_1 r)} H_\theta^{(1)} \quad . \tag{A-4}$$

The E_θ is given by

$$E_\theta^{(1)} = \frac{i\mu_1 \omega}{\lambda_1} J_1(\lambda_1 r)\, b_o^{(1)} F_o \quad . \tag{A-5}$$

Because of the symmetry, $E_\theta^{(1)} = 0$; thus $b_o^{(1)} = 0$. This also nullifies the H_r and H_Z components.

In order to construct a solution appropriate to region 2, the Neumann function portion of the general solution must also be retained. Since[6]

$$\frac{dZ_n(\rho)}{d\rho} = \frac{1}{2} Z_{n-1}(\rho) - \frac{1}{2} Z_{n+1}(\rho) \tag{A-6}$$

and

$$Z_{n-1} + Z_{n+1} = \frac{2n}{\rho} Z_n \quad , \tag{A-7}$$

for Z equal to a Bessel or Neumann function, more general equations equivalent to Eqs. (13) through (18) may be written, including the Hankel functions. The azimuthal component for magnetic field intensity then becomes

$$H_\theta(2) = \frac{-ik_2^2}{\omega\mu_2\lambda_2} \left[A\, J_1(\lambda_2 r) + B\, N_1(\lambda_2 r) \right] e^{ihZ - i\omega t} \quad , \tag{A-8}$$

as given by Stratton.[2] From the more general equations equivalent to (13) through (18), one finds

$$E_r(2) = \frac{\omega\mu_2 h}{k_2^2} H_\theta(2) \quad , \tag{A-9}$$

$$E_Z(2) = - \frac{\omega\mu_2\lambda_2}{ik_2^2} \frac{A\, J_o(\lambda_2 r) + B\, N_o(\lambda_2 r)}{A\, J_1(\lambda_2 r) + B\, N_1(\lambda_2 r)} H_\theta(2) \quad . \tag{A-10}$$

In a similar manner, in region 3 the functions are combined so that only the Hankel function is retained for proper behavior at infinity:

$$H_\theta(3) = - \frac{ik_3^2}{\omega\mu_3\lambda_3} C\, H_1^{(1)}(\lambda_3 r)\, e^{ihZ - i\omega t} \quad , \tag{A-11}$$

$$E_r(3) = \frac{\omega\mu_3 h}{k_3^2} H_\theta(3) \quad , \tag{A-12}$$

$$E_Z(3) = - \frac{\omega\mu_3\lambda_3}{ik_3^2} \frac{H_o^{(3)}(\lambda_3 r)}{H_1^{(3)}(\lambda_3 r)} H_\theta(3) \quad . \tag{A-13}$$

The constants A, B, and C are determined by the boundary conditions, continuity of E_Z and H_θ at $r = a_1$ and a_2. As given in Stratton, these boundary conditions determine the ratio of A and B as

$$-\frac{A}{B} = \frac{N_o(\lambda_2 a_1) - \frac{\mu_1\lambda_1 k_2^2}{\mu_2\lambda_2 k_1^2}\frac{J_o(\lambda_1 a_1)}{J_1(\lambda_1 a_1)} N_1(\lambda_2 a_1)}{J_o(\lambda_2 a_1) - \frac{\mu_1\lambda_1 k_2^2}{\mu_2\lambda_2 k_1^2}\frac{J_o(\lambda_1 a_1)}{J_1(\lambda_1 a_1)} J_1(\lambda_2 a_1)} \tag{A-14}$$

$$= \frac{N_o(\lambda_2 a_2) - \frac{\mu_3\lambda_3 k_2^2}{\mu_2\lambda_2 k_3^2}\frac{H_o^{(1)}(\lambda_3 a_2)}{H_o^{(1)}(\lambda_3 a_2)} N_1(\lambda_2 a_2)}{J_o(\lambda_2 a_2) - \frac{\mu_3\lambda_3 k_2^2}{\mu_2\lambda_2 k_3^2}\frac{H_o^{(1)}(\lambda_3 a_2)}{H_1^{(1)}(\lambda_3 a_2)} J_1(\lambda_2 a_2)} \quad . \tag{A-15}$$

The values of $h = \sqrt{k_i^2 - \lambda_i^2}$, which are the roots of this determinantal equation, fix the allowed modes of propagation.

Consider the case where the inner and outer regions are of infinite conductivity. Since

$$\lambda^2 = k^2 - h^2, \tag{A-16}$$

where

$$k^2 = \omega^2\mu\varepsilon + i\omega\mu\sigma, \tag{A-17}$$

the conductivity term dominates in regions 1 and 3. For $\ell = 1, 3$,

$$k_\ell^2 = i\omega\mu_\ell\sigma_\ell \ , \tag{A-18}$$

$$\lambda_\ell^2 = i\omega\mu_\ell\sigma_\ell - h^2. \tag{A-19}$$

Since the imaginary part of h must remain finite for propagation of the wave as conductivity becomes large,

$$\lambda_\ell \approx k_\ell \approx \sqrt{i\omega\mu_\ell\sigma_\ell} \ . \tag{A-20}$$

Because of the k_ℓ^2 term, Eqs. (A-14) and (A-15) become

$$\frac{N_o(\lambda_2 a_1)}{J_o(\lambda_2 a_1)} = \frac{N_o(\lambda_2 a_2)}{J_o(\lambda_2 a_2)} \quad . \tag{A-21}$$

The λ_2 values which satisfy (A-21) determine the propagation constant via (A-16). One obvious solution is $\lambda_2 = 0$, corresponding to $h = k_2$, a wave the propagation constant of which is that of the medium between the two conducting cylinders.

From (A-16), when λ_2^2 becomes large, h^2 becomes imaginary, and such waves are rapidly attenuated. Let us consider the $\lambda_2 \approx 0$ mode of propagation further. For

$$x \ll 1 \quad , \quad J_1(x) \approx \frac{1}{\Gamma(2)} \left(\frac{x}{2}\right) \quad , \quad N_1(x) \approx -\frac{\Gamma(1)}{\pi} \left(\frac{2}{x}\right) \quad ,$$

and (A-8) becomes

$$H_\theta^{(2)} = \frac{ik_2^2}{\mu_2 \omega} \left[\frac{-Ar}{2} + \frac{2B}{\pi \lambda_2^2 r} \right] e^{\left(ik_2 Z - i\omega t\right)} \quad . \tag{A-22}$$

For reasonably small r and small λ_2 the B term must dominate. The B may be evaluated in terms of the current in the center conductor by using Ampere's law. Thus

$$\oint_C \underline{H} \cdot d\underline{\ell} = I = 2\pi a_1 H_\theta^{(2)} \quad , \tag{A-23}$$

$$B = \frac{-i \omega \mu_2 \lambda_2^2 I_o}{4k_2^2} \quad . \tag{A-24}$$

Now,

$$H_\theta^{(2)} = \frac{I}{2\pi r} \quad , \tag{A-25}$$

and from Eqs. (A-9) and (A-10),

$$E_r^{(2)} = \frac{\omega \mu_2}{2\pi k_2} \frac{I}{r} , \quad E_Z^{(2)} = 0 . \tag{A-26}$$

With a finite conductivity in regions 1 and 3, the propagation factors must be modified to account for added attenuation. With the assumption that λ_2 is still small,

$$N_o(\lambda_2 a_1) \approx + \frac{2}{\pi} \ell n \frac{\lambda_2 a_1}{2} + 0.5772 , \tag{A-27}$$

$$N_1(\lambda_2 a_1) \approx - \frac{2}{\pi \lambda_2 a_1} ; \tag{A-28}$$

$$k_\ell^2 \approx i \omega \mu_\ell \sigma_\ell , \quad \ell = 1, 3 . \tag{A-29}$$

Because of the large σ_ℓ, the denominators in (A-14) and (A-15) are unity, and the numerators may be simplified to

$$- \frac{A}{B} \frac{\pi}{2} \approx \ell n \frac{\lambda_2 a_1}{2} + 0.5772 + \frac{k_2^2}{\mu_2 \lambda_2^2} \sqrt{\frac{\mu_1}{i\omega\sigma_1}} \frac{1}{a_1} \frac{J_o(\lambda_1 a_1)}{J_1(\lambda_1 a_1)} \tag{A-30}$$

and also

$$\approx \ell n \frac{\lambda_2 a_2}{2} + 0.5772 + \frac{k_2^2}{\mu_2 \lambda_2^2} \sqrt{\frac{\mu_3}{i\omega\sigma_3}} \frac{1}{a_2} \frac{H_o^{(1)}(\lambda_3 a_2)}{H_1^{(1)}(\lambda_3 a_2)} . \tag{A-31}$$

This requires that

$$\lambda_2^2 = \frac{k_2^2}{\mu_2 \ell n(a_2/a_1)} \left\{ \sqrt{\frac{\mu_3}{i\omega\sigma_3 a_2^2}} \frac{H_o^{(1)}(\lambda_3 a_2)}{H_1^{(1)}(\lambda_3 a_2)} - \sqrt{\frac{\mu_1}{i\omega\sigma_1 a_1^2}} \frac{J_o(\lambda_1 a_1)}{J_1(\lambda_1 a_1)} \right\} . \tag{A-32}$$

In terms of the propagation constant h, since $\lambda_2 \ll h$,

$$h^2 = k_2^2 - \lambda_2^2, \qquad h \approx k_2 + i\,\lambda_2^2/2k_2 \quad , \tag{A-33}$$

$$h = k_2 + \frac{ik_2}{2\mu_2\,\ell n(a_2/a_1)} \left\{ \sqrt{\frac{\mu_3}{i\omega\sigma_3\,a_2^2}}\; \frac{H_o^{(1)}(\sqrt{i\omega\mu_3\sigma_3}\;a_2)}{H_1^{(1)}(\sqrt{i\omega\mu_3\sigma_3}\;a_2)} \right. \tag{A-34}$$

$$\left. - \sqrt{\frac{\mu_1}{i\omega\sigma_1\,a_1^2}}\; \frac{J_o\,(\sqrt{i\omega\mu_1\sigma_1}\;a_1)}{J_1\,(\sqrt{i\omega\mu_1\sigma_1}\;a_1)} \right\} \quad ,$$

$$h = k_2\,(1 + \alpha) \quad . \tag{A-35}$$

The α term is small because of the high conductivities in regions 1 and 3.

With the determination of h, (A-8) gives the azimuthal magnetic field in region 2. After the approximation $\lambda_2\, r \ll 1$ is applied together with substitution for A from (A-30),

$$H_\theta^{(2)} = + \frac{2ik_2^2\,B}{\pi\omega\mu_2\,\lambda_2^2} \left\{ \left[a_1\lambda_2^2 \left(\ell n\, \frac{\lambda_2\, a_1}{2} + 0.5772 \right) + \frac{k_2^2}{\mu_2} \sqrt{\frac{\mu_1}{i\omega\sigma_1}} \right.\right.$$

$$\left.\left. \cdot\, \frac{J_o(\lambda_1\, a_1)}{J_1(\lambda_1\, a_1)} \right] \frac{r}{2a_1} + \frac{1}{r} \right\} e^{ihZ - i\omega t} \quad . \tag{A-36}$$

The λ_2^2 term in the numerator is neglected, since λ_2 is small.

APPENDIX B

MATHEMATICAL DETAILS OF THE DIFFRACTION PROBLEM FOR THE COAXIAL CABLE MODEL

APPENDIX B

MATHEMATICAL DETAILS OF THE DIFFRACTION PROBLEM FOR THE COAXIAL CABLE MODEL

The Fourier transform of each component of the electromagnetic field in a vacuum satisfies the Helmholtz equation

$$(\nabla^2 + k^2)\, U = 0, \tag{B-1}$$

where $k = \omega/c$. The solution at (x,y,z) is

$$U(\vec{r}) = \frac{1}{4\pi} \iint_S \left\{ U(\vec{r}') \frac{\partial}{\partial n'} \left(\frac{e^{ik|\vec{r}-\vec{r}'|}}{|\vec{r}-\vec{r}'|} \right) - \frac{e^{ik|\vec{r}-\vec{r}'|}}{|\vec{r}-\vec{r}'|} \frac{\partial U}{\partial n'} \right\} dS', \tag{B-2}$$

where n' is the unit normal directed inward with respect to the surface of integration. In the special case considered here, the fields on S' are negligible everywhere except $a_1 \le r \le a_2$ on the $z' = 0$ plane. The radius vector notation used here is $\underline{r} = (r, \varphi, z)$. Recall that the $z = 0$ plane is the interface between the earth and air.

Then

$$|\underline{r}-\underline{r}'|^2 = r^2 + r'^2 - 2rr \cos(\varphi-\varphi') + z^2 + z'^2 - 2zz', \tag{B-3}$$

$$\frac{\partial}{\partial z'} |\underline{r}-\underline{r}'| = \frac{z'-z}{\left[r^2+r'^2 - 2rr' \cos(\varphi-\varphi') + z^2 + z'^2 - 2zz'\right]^{1/2}}. \tag{B-4}$$

Substitution into (B-2) gives

$$U(r,0,0) = \frac{1}{4\pi} \int_0^{2\pi} d\varphi' \int_{a_1}^{a_2} r'\, dr' \left[U(r',0,0)\, e^{ik|\underline{r}-\underline{r}'|} \right.$$

$$\left. \left\{ \frac{ik \frac{\partial}{\partial z'} |\underline{r}-\underline{r}'|}{|\underline{r}-\underline{r}'|} - \frac{\frac{\partial}{\partial z'} |\underline{r}-\underline{r}'|}{|r-r'|^2} \right\} - \frac{e^{ik|\underline{r}-\underline{r}'|}}{|\underline{r}-\underline{r}'|} \frac{\partial U}{\partial z'} \Bigg|_{z'=0} \right]. \tag{B-5}$$

The terms involving $\frac{\partial}{\partial z'} |\underline{r}-\underline{r}'|$ are zero for the observer on the z = 0 plane; thus

$$U(r,0,0) = \frac{-1}{4\pi} \int_0^{2\pi} d\varphi' \int_{a_1}^{a_2} r'dr' \left[\frac{e^{ik|\underline{r}-\underline{r}'|}}{|\underline{r}-\underline{r}'|} \frac{\partial U}{\partial z'}\Big|_{z'=0} \right]. \tag{B-6}$$

With the assumption that r >> r', for z = z' = 0,

$$\frac{e^{ik|\underline{r}-\underline{r}'|}}{|\underline{r}-\underline{r}'|} \approx \frac{e^{ikr}}{r} \exp\left[- ikr' \cos \varphi' \right] . \tag{B-7}$$

Thus

$$U(r,0,0) = - \frac{e^{ikr}}{4\pi r} \int_0^{2\pi} d\varphi' \int_{a_1}^{a_2} r' \, dr' \exp\left[-ikr' \cos \varphi'\right] \frac{\partial U}{\partial z'}\Big|_{z'=0}. \tag{B-8}$$

Let $U = H_\varphi$. When one assumes that the upper half space has $\underline{J} = 0$ and $H_r = H_z = 0$,

$$\nabla \times \underline{H} = - i\omega\varepsilon_o \underline{E}, = - \frac{\partial H_\varphi}{\partial z} \hat{e}_r + \frac{1}{r} \frac{\partial}{\partial r} (r H_\varphi) \hat{e}_z . \tag{B-9}$$

The wave may be approximated as a radiating wave in the upper half space. Hence

$$\frac{\partial}{\partial r'} (r'H_{\varphi'}) \approx 0 \tag{B-10}$$

and

$$\frac{\partial H_{\varphi'}(r')}{\partial z'} = i\omega\varepsilon_o E_{r'}(r') . \tag{B-11}$$

Thus from Eq. (B-8),

$$H_\varphi(r,0,0) = - \frac{e^{ikr}}{4\pi r} \int_0^{2\pi} d\varphi' \int_{a_1}^{a_2} r'dr'$$

$$x \exp\left[-ikr' \cos \varphi' \right] i\omega\varepsilon_o E_{r'}(r') \cos \varphi' \Big|_{z'=0} . \tag{B-12}$$

The factor cos φ' ($\varphi = 0$ for chosen observer) is introduced, since only the $\hat{e}_r$ component of $E_{r'}$, $\hat{e}_{r'}$, contributes to H_φ.

In the radiation zone, then, for observers on the z = 0 plane,

$$H_\varphi(r,0,0) = - \frac{i\omega\epsilon_o e^{ikr}}{4\pi r} \int_{a_1}^{a_2} E_{r'}(r')r'dr' \int_o^{2\pi} \exp\left[-ikr'\cos\varphi'\right] \times \cos\varphi' \, d\varphi' \quad . \tag{B-13}$$

The identity[7]

$$J_m(Z) = \frac{(-i)^m}{\pi} \int_o^{\pi} e^{iz\cos t} \cos mt \, dt \tag{B-14}$$

gives

$$- \frac{\pi}{i}\left[J_1(-kr') - J_1(kr')\right] = \int_o^{2\pi} e^{-ikr'\cos t} \cos t \, dt \tag{B-15}$$

$$= \frac{2\pi}{i} J_1(kr'),$$

since $J_1(-z) = - J_1(z)$.

Thus

$$H_\phi(r,0,0) = - \frac{\omega\epsilon_o e^{ikr}}{2r} \int_{a_1}^{a_2} E_{r'}(r')r' \, J_1(kr') \, dr'. \tag{B-16}$$

The source term from the coaxial cable model is given in Eq. (44) for the special case in Section III:

$$E_{r'}(r') = \frac{G}{r'} \quad , \tag{B-17}$$

where

$$G = \frac{2 \; 10^{-7} \; I_o \exp\left[\, i\omega(A_1 Z - t)\right] \exp\left[-\omega B_1 Z\right]}{(A_1 + iB_1)} \, . \tag{B-18}$$

Thus

$$H_{\varphi}(r,0,0) = - \frac{\omega \epsilon_o \, e^{ikr}}{2r} G \int_{a_1}^{a_2} J_1(kr') \, dr' \, . \qquad \text{(B-19)}$$

Since[7]

$$J_o'(z) = - J_1(z),$$

$$H_{\varphi}(r,0,0) = \frac{\omega \epsilon_o \, e^{ikr} G}{2kr} \left[J_o(ka_2) - J_o(ka_1) \right] . \qquad \text{(B-20)}$$

For the radiation zone,

$$E_z = - \mu_o c \, H_{\varphi} \, . \qquad \text{(B-21)}$$

Thus the radiating vertical component of electric field intensity is

$$E_z = - \frac{e^{ikr} G}{2r} \left[J_o(ka_2) - J_o(ka_1) \right] \, . \qquad \text{(B-22)}$$

APPENDIX C

MATHEMATICAL DETAILS OF THE UNDERGROUND ANTENNA MODEL

APPENDIX C

MATHEMATICAL DETAILS OF THE UNDERGROUND ANTENNA MODEL

Let space be divided into two regions: Region I has $0 \leq r \leq a_1$, whereas region II has $r > a_1$. The r is the distance from the z axis in a cylindrical coordinate system. Region I is assumed to be a good conductor, while region II is the earth (which probably should not be referred to as ground). Azimuthal symmetry is assumed, so much of the earlier treatment applies. In region II, however, only the Hankel function can be retained for proper behavior at large distances. In analogy with Eqs. (A-11) through (A-13),

$$H_\theta^{(2)} = \frac{-ik_2^2}{\omega\mu_2\lambda_2} \, C \, H_1^{(1)}(\lambda_2 r) \exp(ihZ), \tag{C-1}$$

$$E_r^{(2)} = \frac{\omega\mu_2 h}{k_2^2} \, H_\theta^{(2)}, \tag{C-2}$$

$$E_z^{(2)} = \frac{-\omega\mu_2\lambda_2}{ik_2^2} \frac{H_o^{(1)}(\lambda_2 r)}{H_1^{(1)}(\lambda_2 r)} \, H_\theta^{(2)} . \tag{C-3}$$

From (A-2) - (A-4),

$$H_\theta^{(1)} = \frac{ik_1^2 I}{2\pi a_1 \omega\mu_1\sigma_1} \frac{J_1(\lambda_1 r)}{J_1(\lambda_1 a_1)}, \tag{C-4}$$

$$E_r^{(1)} = \frac{\omega\mu_1 h}{k_1^2} \, H_\theta^{(1)} , \tag{C-5}$$

$$E_z^{(1)} = \frac{-\omega\mu_1\lambda_1}{ik_1^2} \frac{J_o(\lambda_1 r)}{J_1(\lambda_1 r)} \, H_\theta^{(1)} , \tag{C-6}$$

where $I = I_o e^{ihZ}$ is the Fourier transform of the current. H_θ is continuous at $r = a_1$. Thus:

$$\frac{-i\ k_2^2}{\mu_2 \lambda_2} C\ H_1^{(1)}(\lambda_2 a_1) = \frac{ik_1^2\ I_o}{2\pi a_1 \mu_1 \sigma_1} \quad , \tag{C-7}$$

or

$$C = \frac{-k_1^2\ I_o \mu_2 \lambda_2}{k_2^2\ 2\pi a_1 \sigma_1 \mu_1 H_1^{(1)}(\lambda_2 a_1)} \quad . \tag{C-8}$$

Substitution into (C-1) yields

$$H_\theta^{(2)} = \frac{ik_1^2\ I_o H_1^{(1)}(\lambda_2 r) e^{ihZ}}{2\pi\ \omega a_1 \sigma_1 \mu_1 H_1^{(1)}(\lambda_2 a_1)} \quad . \tag{C-9}$$

Recall that

$$h^2 = k_2^2 - \lambda_2^2 = k_1^2 - \lambda_1^2, \tag{C-10}$$

$$k_j^2 = \omega^2 \mu_j \epsilon_j + i\omega\mu_j\sigma_j, \tag{C-11}$$

$$k_1^2 \approx i\omega\mu_1\sigma_1 \ ; \tag{C-12}$$

therefore,

$$\lambda_1^2 = i\omega\mu_1\sigma_1 - h^2 \quad . \tag{C-13}$$

Since $\sigma_1 \to \infty$, the imaginary part of h must remain finite for propagation of the wave. Thus

$$\lambda_1 = k_1 = \sqrt{i\omega\mu_1\sigma_1} \quad . \tag{C-14}$$

The second boundary condition is continuity of E_z. This leads to

$$\frac{\mu_2\lambda_2}{k_2^2} \frac{H_o^{(1)}(\lambda_2 a_1)}{H_1^{(1)}(\lambda_2 a_1)} = \frac{\mu_1\lambda_1}{k_1^2} \frac{J_o(\lambda_1 a_1)}{J_1(\lambda_1 a_1)} \quad . \tag{C-15}$$

The propagation factor h is determined from solution of (C-15). If region I has infinite conductivity, $h = k_2$. For large conductivity

$$h \approx k_2 \quad . \tag{C-16}$$

The term

$$\lambda_2 = \sqrt{k_2^2 - h^2} \tag{C-17}$$

is a small quantity. Thus

$$\frac{H_o^{(1)}(\lambda_2 a_1)}{H_1^{(1)}(\lambda_2 a_1)} \approx -\lambda_2 a_1 \ln\left\{\frac{1.781\ \lambda_2 a_1}{2i}\right\}. \tag{C-18}$$

Since

$$\lambda_1^2 \approx i\omega\mu_1\sigma_1 \approx 4\pi i\omega \ , \tag{C-19}$$

with $\sigma_1 = 10^7$ MKS units and $a_1 \approx 1$ m,

$$\left|\lambda_1 a_1\right| \approx \left|\sqrt{4\pi i\omega}\right| >> 1 \ .$$

This indicates the asymptotic limit in (29) can be used for the ratio of Bessel functions. Equation (C-15), determining h, is then

$$\left(\lambda_2 a_1\right)^2 \ln\left(\frac{1.781\lambda_2 a_1}{2i}\right)^2 = \frac{2ik_2^2 a_1}{k_1} \quad . \tag{C-20}$$

From (C-12), $k_1^2 = i\omega\mu_1\sigma_1$, the real and imaginary parts are

$$\left.\begin{matrix} k_{1r} \\ k_{1i} \end{matrix}\right\} = \sqrt{\mu_1\epsilon_1}\ \omega\left[\frac{\sqrt{1+\left(\frac{\sigma_1}{\epsilon_1\omega}\right)^2} \pm 1}{2}\right]^{1/2} , \tag{C-21}$$

or

$$k_1 = (1 + i)\sqrt{\frac{\mu_1\sigma_1\omega}{2}}$$

for the good conductor.

Equation (C-20), determining h (λ_2), is now

$$\frac{1}{2}\left(\lambda_2 a_1\right)^2 \ell n\left(\frac{1.781\lambda_2 a_1}{2i}\right)^2 = \frac{i a_1\left(\omega^2\mu_2\varepsilon_2 + i\omega\mu_2\sigma_2\right)}{(1+i)\sqrt{\frac{\mu_1\sigma_1\omega}{2}}} \quad . \qquad \text{(C-22)}$$

Let $x = \left(\frac{1.781\lambda_2 a_1}{2i}\right)^2$. Then, with the choice of μ_2, ε_2, σ_2, μ_1, σ_1 as in the special case, the equation determining h becomes

$$x\ \ell n\ x = \frac{-(1.781)^2}{\sqrt{16\pi\omega}}\ (1+i)\left[\ 111 \times 10^{-18}\ \omega^2 + i\omega 18.8 \times 10^{-11}\ \right]. \qquad \text{(C-23)}$$

As an example, assume $\omega = 10^9$ sec^{-1}. Then

$$x\ \ell n\ x = -\ 15.72 \times 10^{-4}\ (1+i)\ . \qquad \text{(C-24)}$$

Since the $\ell n\ x$ is a slowly varying function of x, the equation may be solved by an iterative process. One may arbitrarily choose

$$\ell n\ x_o = -\ 5,$$

$$x_1\ \ell n\ x_o = -\ 15.72 \times 10^{-4}\ (1+i) \quad .$$

This yields an estimate for x of

$$x_1 = 3.144\ 10^{-4}\ (1+i).$$

The ℓn of a complex number is given by $\ell n\ (x+iy) = 1/2\ \ell n\ (x^2+y^2) + i\ \tan^{-1} y/x$. Thus

$$\ell n\ x_1 = -\ 7.718 + i\ \pi/4\ .$$

Substitution into Eq. (C-22) again gives a better approximation:

$$x_2 = 1.811 \times 10^{-4} + i\ 2.221 \times 10^{-4}\ ;$$

$$\ell n x_2 = -\ 8.19 + i\ 0.888.$$

The next iteration gives

$$x_3 = 1.690\ 10^{-4} + 2.102\ i\ 10^{-4},$$

$$\ell n\ x_3 = -\ 8.21 + i\ 0.894\ ,$$

and

$$x_4 = (1.686 + i\ 2.098)\ 10^{-4}.$$

The x_4 is reasonably close to x_3, and the iteration is terminated:

$$\left(\frac{1.781\lambda_2 a_1}{2i}\right)^2 = (1.686 + i\ 2.098)\ 10^{-4} \quad . \tag{C-25}$$

The speed of convergence of this method is greatly increased in certain situations if π is added to the phase of $\ell n\ x$ for cases where $\mathrm{Im}(\ell n\ x)$ is less than zero. (Effectively, the arc tan function is allowed to vary from 0 to π rather than the $-\pi/2$ to $\pi/2$ limits utilized by standard computer libraries.) Thus

$$\pm\ \lambda_2 a_1 = (0.797 - i\ 1.66)\ 10^{-2} \quad . \tag{C-26}$$

From Eqs. (C-10), (C-11), and (C-26) with $a_1 = 1$ meter and $\omega = 10^9$,

$$h^2 = 111 + 2.126 \times 10^{-4} + i\left[0.188 + 2.646 \times 10^{-4}\right] , \tag{C-27}$$

$$h^2 \approx k_2{}^2 . \tag{C-28}$$

The change due to λ_2 is negligible. Thus

$$h^2 = 111 + 0.188i. \tag{C-29}$$

The real and imaginary parts (for $\omega = 10^9$) are then

$$h = 10.5 + 0.0090i \quad . \tag{C-30}$$

The phase velocity of the wave propagation is

$$\frac{\omega}{h_r} \approx 10^8 \text{ m/sec.} \tag{C-31}$$

The e folding distance is

$$d_e = 1/\mathrm{Im}(h) = 111 \text{ meters.} \tag{C-32}$$

With the determination of h, the fields are known in region II from (C-2), (C-3), and (C-9).

A check of the approximation $\lambda_2 a_1 \ll 1$ for an ω at the frequency 10^4 Hz to determine if it is valid at the low frequencies of interest gives

$$(\pm)\lambda_2 a_1 = (2.42 - i\ 1.068)\ 10^{-5}\ , \tag{C-33}$$

an even smaller quantity.

The Radial Component of Electric Field Intensity

From Eqs. (C-2) and (C-9),

$$E_r^{(2)} = \frac{i\mu_2 h k_1^2 I_o H_1^{(1)}(\lambda_2 r) e^{ihZ}}{2\pi k_2^2 a_1 \sigma_1 \mu_1 H_1^{(1)}(\lambda_2 a_1)}\ . \tag{C-34}$$

The r dependence resides in the $H_1^{(1)}(\lambda_2 r)$ function. If $|\lambda_2| \approx 10^{-2}$, as estimated for the $\omega = 10^9$ case, then for $r \gg 10^2$ meters, the large argument approximation may be used for $H_1^{(1)}(\lambda_2 r)$:

$$H_1^{(1)}(\lambda_2 r) \approx \sqrt{\frac{2}{\pi \lambda_2 r}}\ e^{i(\lambda_2 r - 3\pi/4)}\ . \tag{C-35}$$

In $(\pm)\lambda_2 \approx (0.797 - i\ 1.66)\ 10^{-2}$, only the negative sign may be retained so that the radial component of E will reduce as $e^{-1.66 \times 10^{-2} r/\sqrt{r}}$ rather than having a term growing exponentially with distance. One might look for an r dependence of the E_r varying as $\frac{e^{-\alpha r}}{\sqrt{r}}$ for this frequency and choice of parameters.

The Radiated Field

Judging from the radial part, one must go reasonably far from the antenna to be out of the source region on the "z" = o plane for calculation of the radiated fields. With the assumption of r >> r', Eq. (B-16) applies, and

$$H_\phi(r_1 0_1 0) = \frac{-\omega\epsilon_o \exp(ikr)}{2r} \int_{a_1}^{\infty} E_{r'}(r')r'J_1(kr')dr'. \qquad \text{(C-36)}$$

The value $E_r(r')$ is available from (C-34), and in the radiation zone

$$E_z = -\mu_o c H_\phi . \qquad \text{(C-37)}$$

Combining yields

$$E_z = \frac{c\omega\mu_o\epsilon_o \exp(ikr)}{2r} \frac{\mu_2 h i k_1^2 I_o \exp(ihZ)}{k_2^2 2\pi a_1 \sigma_1 \mu_1 H_1^{(1)}(\lambda_2 a_1)} \int_{a_1}^{\infty} r'J_1(kr')H_1^{(1)}(\lambda_2 r')dr' . \qquad \text{(C-38)}$$

The integral may be evaluated from the identity[8]

$$\int rZ_p(\alpha r)B_p(\beta r)dr = \frac{\beta r Z_p(\alpha r)B_{p-1}(\beta r) - \alpha r Z_{p-1}(\alpha r)B_p(\beta r)}{\alpha^2 - \beta^2} , \qquad \text{(C-39)}$$

where Z and B represent arbitrary Bessel functions.

Hence

$$\int_{a_1}^{\infty} r'J_1(kr')H_1^{(1)}(\lambda_2 r')dr' = \frac{ka_1 H_1^{(1)}(\lambda_2 a_1)J_o(ka_1) - \lambda_2 a_1 H_o^{(1)}(\lambda_2 a_1)J_1(ka_1)}{\lambda_2^2 - k^2} . \qquad \text{(C-40)}$$

Now

$$E_z = \frac{ic\epsilon_o\mu_2 I_o}{4\pi\sigma_1} \frac{\omega \exp(ikr + ihZ)\, hk_1^2 C_1}{k_2^2 r}, \qquad \text{(C-41)}$$

where

$$C_1 = \frac{kJ_o(ka_1)}{k^2 - \lambda_2^2} - \frac{\lambda_2 H_o^{(1)}(\lambda_2 a_1) J_1(ka_1)}{(k^2 - \lambda_2^2) H_1^{(1)}(\lambda_2 a_1)} \quad . \tag{C-42}$$

The small argument approximation for the Hankel functions from (C-18) gives

$$C_1 \approx \frac{kJ_o(ka_1)}{k^2 - \lambda_2^2} + \frac{\lambda_2^2 a_1 J_1(ka_1)}{k^2 - \lambda_2^2} \ln\left(\frac{1.781\lambda_2 a_1}{2i}\right). \tag{C-43}$$

APPENDIX D

GRAPHS OF RADIAL AND VERTICAL COMPONENTS OF ELECTRIC FIELD INTENSITY

APPENDIX D

GRAPHS OF RADIAL AND VERTICAL COMPONENTS OF ELECTRIC FIELD INTENSITY

(These are at 100 meters from ground zero for several choices of earth parameters in the special case of Section VI.)

The results of assuming earth conductivities of 1.5×10^{-4}, 2×10^{-3}, and 2×10^{-2} mho/m are presented in this appendix. The graphs suggest that the waveforms are independent of the dielectric constant (K) of the earth when $\sigma_g \geq 2 \times 10^{-3}$ mho/m.

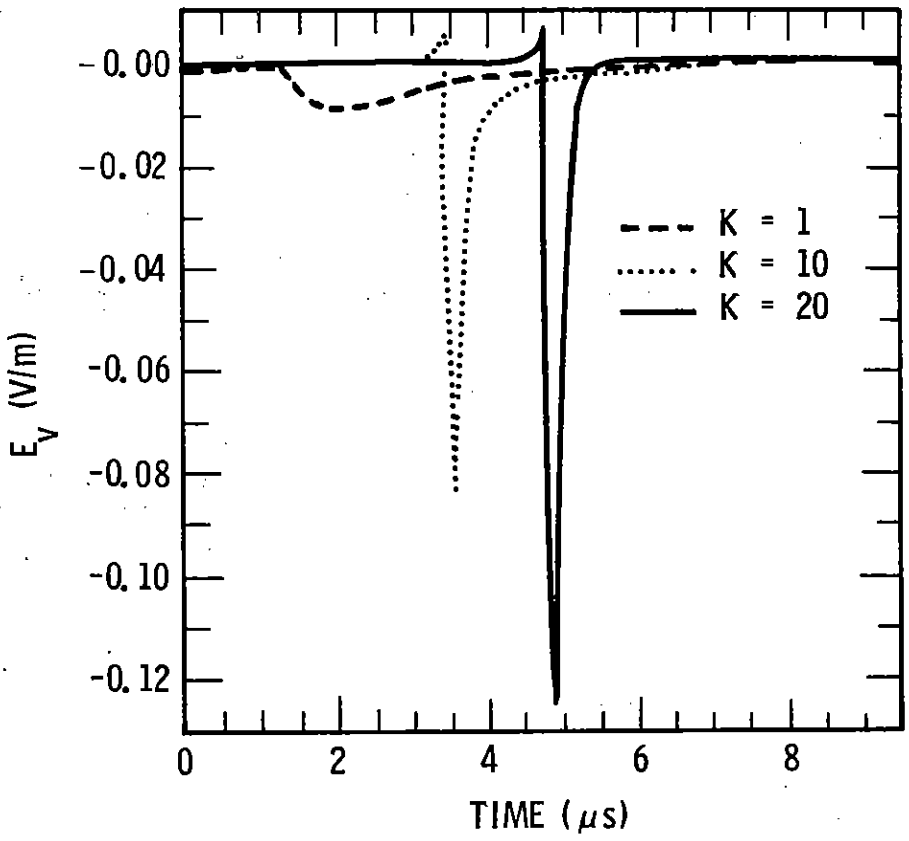

Fig. D-1 Variation of vertical field intensity with earth dielectric constant for a ground conductivity of 1.5×10^{-4} mho/m. The small positive excursions before the negative signals are believed to result from the Fourier transform parameters used rather than reality.

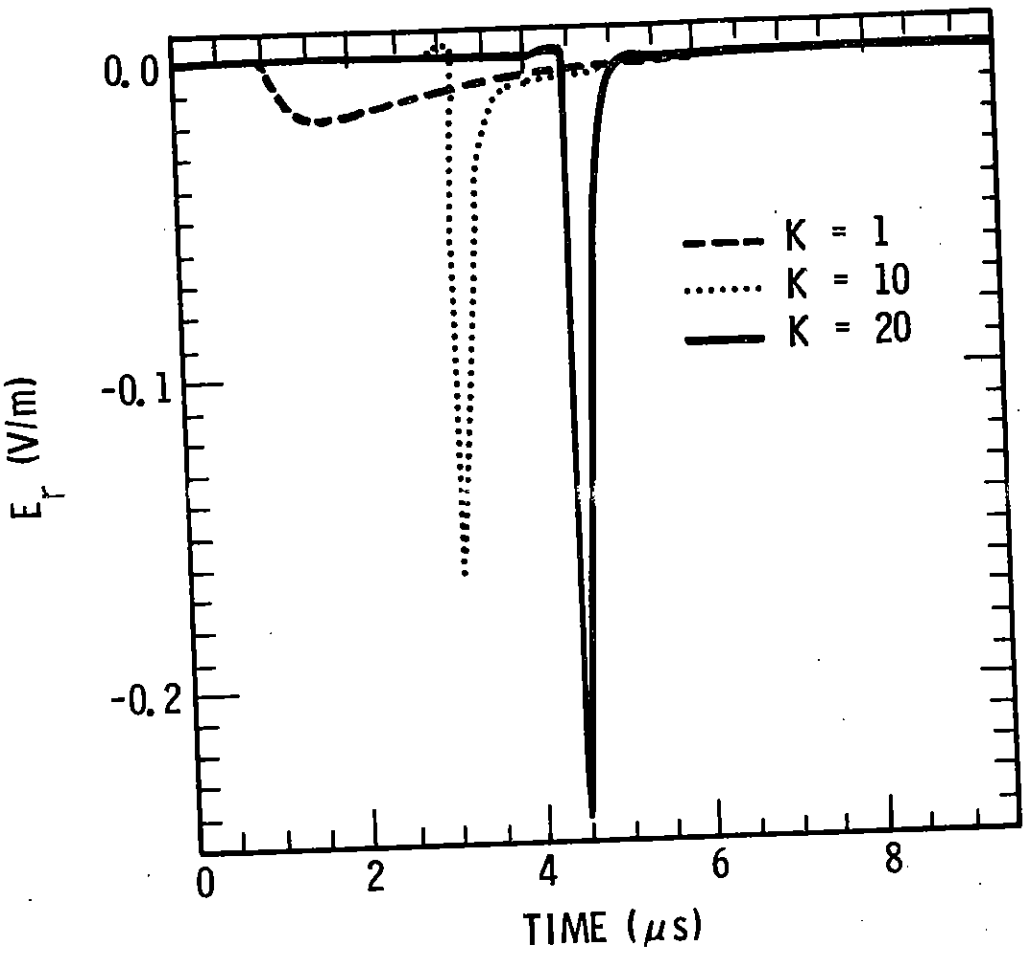

Fig. D-2 Variation of radial electric field intensity with earth dielectric constant for a ground conductivity of 1.5×10^{-4} mho/m.

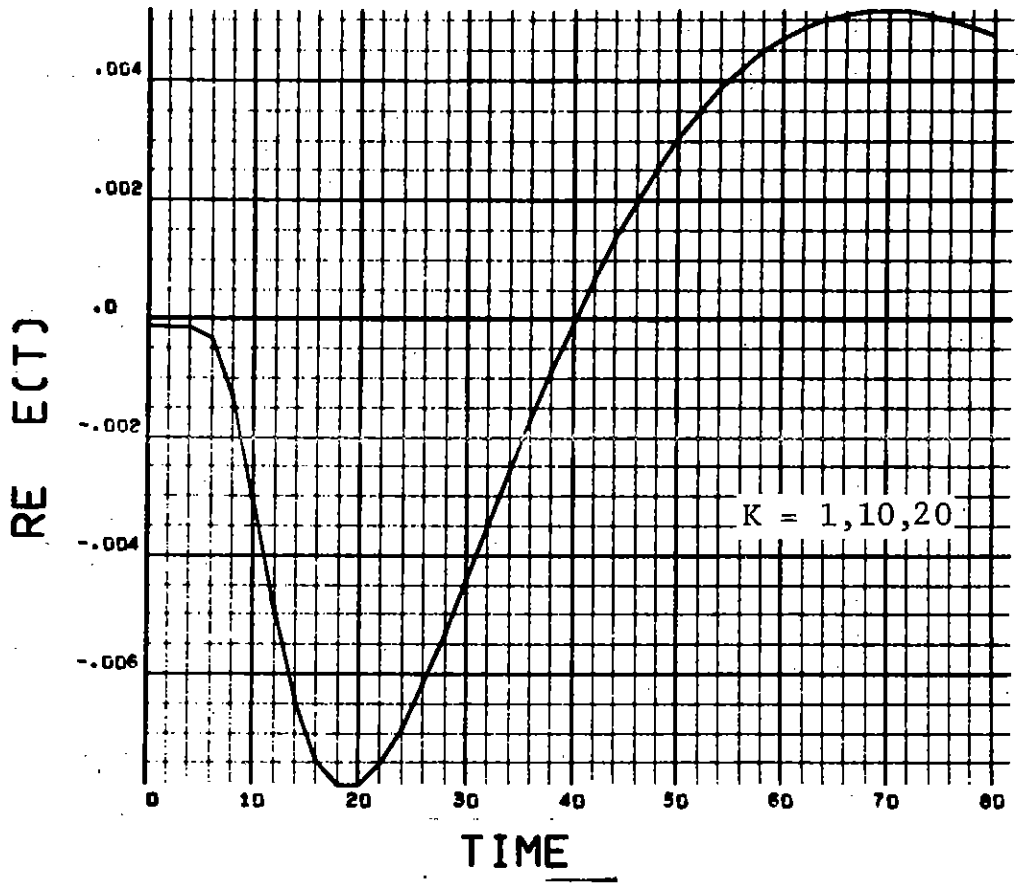

Fig. D-3 Variation of vertical field intensity (V/m) versus time (μs) with earth dielectric constant for a ground conductivity of 2×10^{-3} mho/m.

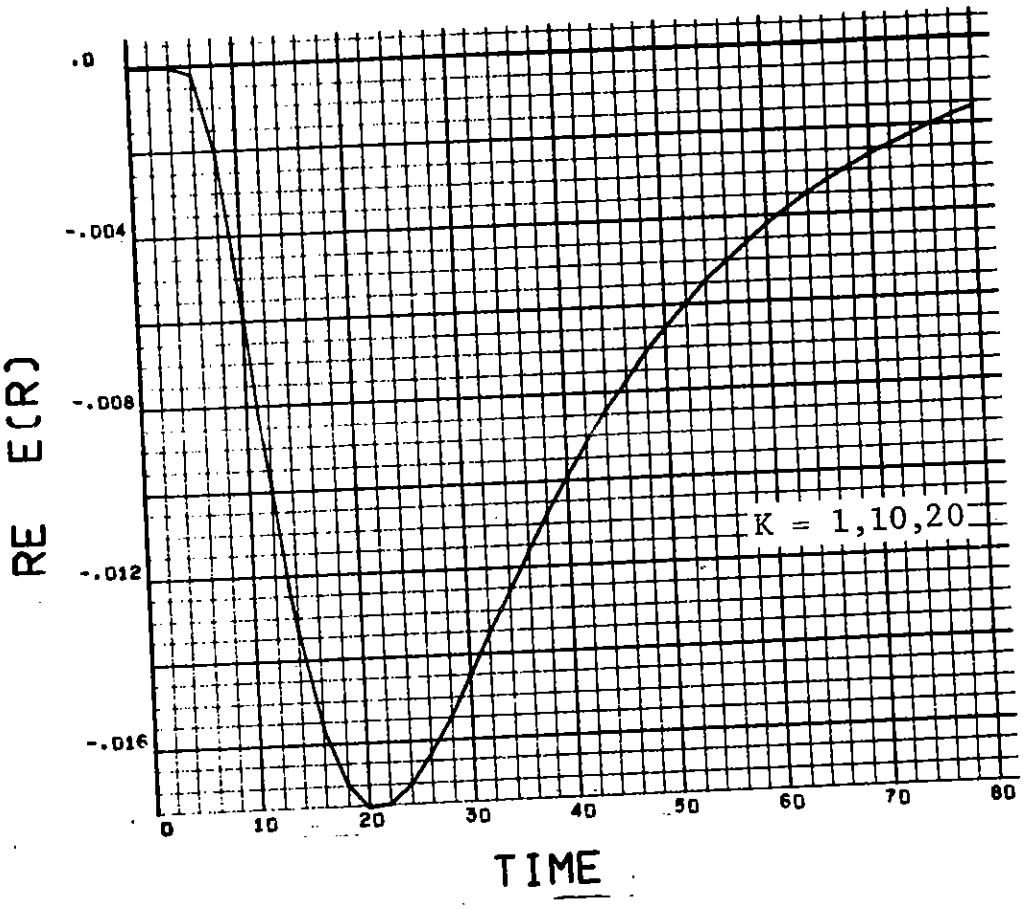

Fig. D-4 Variation of radial field intensity (V/m) versus time (μs) with earth dielectric constant for a ground conductivity of 2×10^{-3} mho/m.

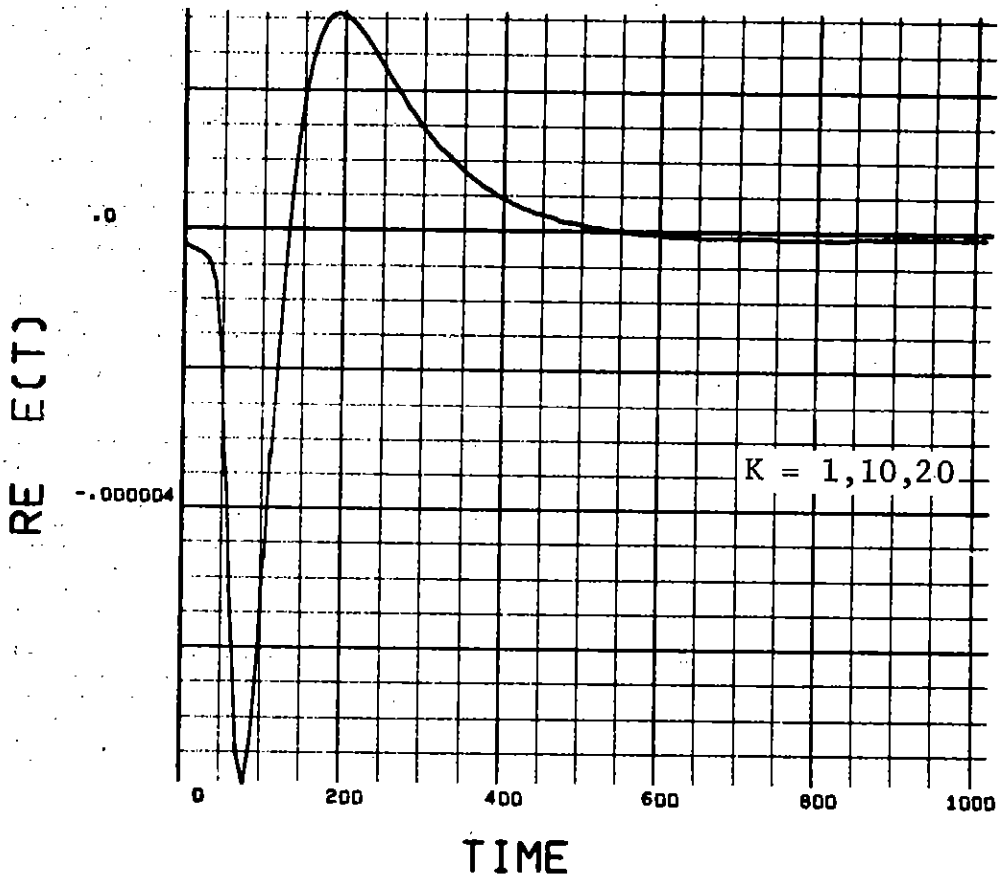

Fig. D-5 Variation of vertical field intensity (V/m) versus time (μs) with earth dielectric constant for a ground conductivity of 2×10^{-2} mho/m.

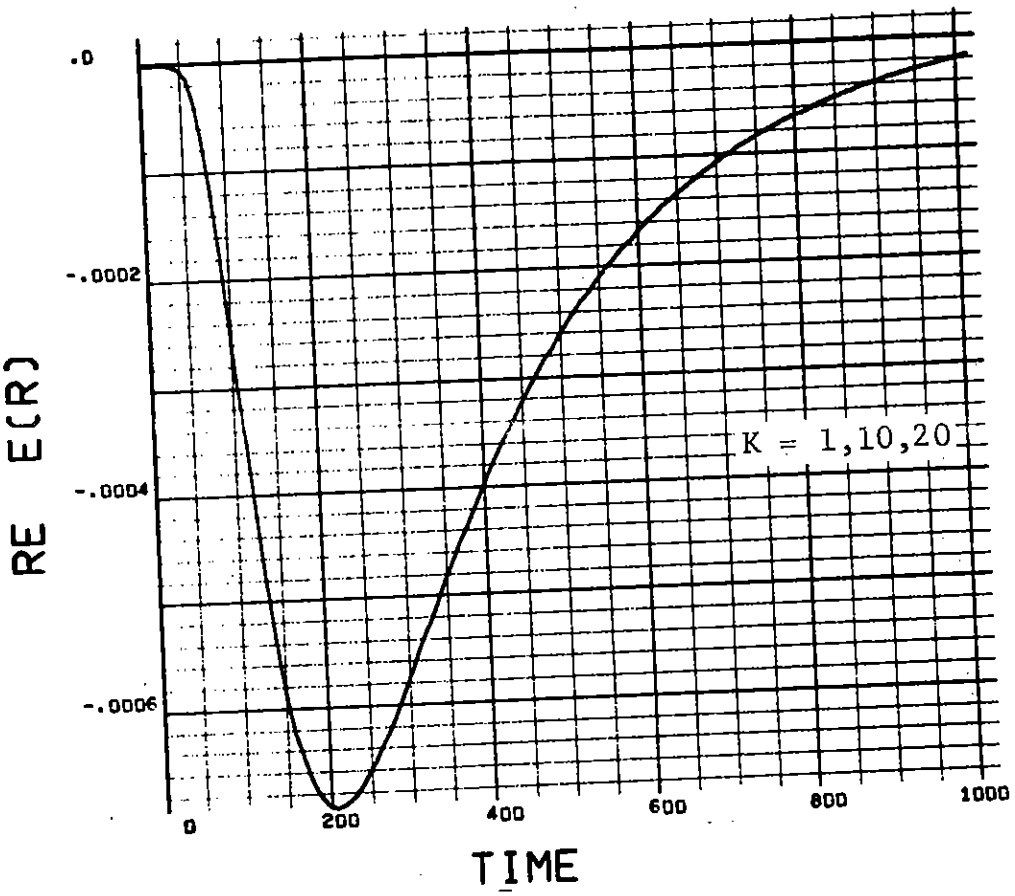

Fig. D-6 Variation of radial field intensity (V/m) versus time (μs) with earth dielectric constant for a ground conductivity of 2×10^{-2} mho/m.

REFERENCES

1. Janis Galejs, Antennas in Inhomogeneous Media, Pergamon Press, New York, 1969, p. 70.

2. Julius A. Stratton, Electromagnetic Theory, McGraw-Hill, New York, 1941, pp. 349, 524. Note the typing error in Stratton's Eq. (8), p. 547, by comparing with Eq. (36) in this report.

3. M. Born and E. Wolf, Principles of Optics, 3rd Edition, Section 8.3, Pergamon Press, New York, 1965.

4. N. M. Brenner, FOURT, Lincoln Laboratory Internal Memorandum. This routine was modified by Rondall Jones of Sandia Laboratories, February 1969.

5. R. D. Halbgewachs, BES: A Routine for the Evaluation of Cylindrical Bessel Functions, SC-M-69-336, Sandia Laboratories, October 1969. Also, see R. D. Halbgewachs, Developments in Techniques for Computation of Bessel Functions by Digital Computers, SC-M-70-3, Sandia Laboratories, February 1970.

6. Handbook of Mathematical Functions of the National Bureau of Standards, edited by M. Abramowitz and I. A. Stegun, 1964.

7. G. A. Korn and T. M. Korn, Mathematical Handbook for Scientists and Engineers, McGraw-Hill, New York, 1968.

8. I. S. Gradshteyn and I. M. Ryzhik, Table of Integrals, Series, and Products, Academic Press, 1965, p. 634.